November 2017

Electroplating on 3D Printed Conductive Track

Kishore Kumar Kadari
University of South Florida, kishorekumar.ls59@gmail.com

Electroplating on 3D Printed Conductive Track

by

Kishore Kumar Kadari

A thesis submitted in partial fulfillment
of the requirements for the degree of
Master of Science in Electrical Engineering
Department of Electrical Engineering
College of Engineering
University of South Florida

Co-Major Professor: Arash Takshi, Ph.D.
Co-Major Professor: Rudy Schlaf, Ph.D.
Jing Wang, Ph.D.

Date of Approval:
October 23, 2017

Keywords: Electrodeposition, Copper, Conductivity, Electronics, PLA

DEDICATION

I dedicate this work to my professor, Dr. Arash Takshi and to my parents.

ACKNOWLEDGEMENTS

Firstly, I express my gratitude to Dr. Arash Takshi. He consistently guided me through my Master's degree. I also convey my thankfulness to Dr. Rudy Schlaf and Dr. Jing Wang for their whole-hearted support.

I thank Dr. Michael Celestin for his help with 3D printers. I truly appreciate Richard Everly for his help at Nanotechnology Research Education Center (NREC), USF.

All my love and thanks to my father Kadari Balram and my mother Kadari Padma for their motivation and love. I thank my colleagues Sabrina Rosa, Fatemeh Khorromshahi, Radwan Elzein for their guidance. I also thank my dear friends Ravi Shanmugha Preethi Vangapattu and Kavya Attaluri for their help in my hard times.

TABLE OF CONTENTS

LIST OF TABLES iii

LIST OF FIGURES iv

ABSTRACT vi

CHAPTER 1: INTRODUCTION 1

CHAPTER 2: BACKGROUND 2
- 2.1 Additive Manufacturing 2
  - 2.1.1 Market Growth in 3D Printing and its Applications 2
  - 2.1.2 Fused Deposition Modeling 3
  - 2.1.3 Conductive PLA 4
- 2.2 Electroplating 5

CHAPTER 3: EQUIPMENT DESCRIPTION AND MATERIALS PREPARATION 9
- 3.1 Keithley 2602A System Source Meter 9
- 3.2 Scanning Electron Microscopy 9
- 3.3 Profiling System 9
- 3.4 $CuSO_4$ Solution 9
- 3.5 Copper Wire, Copper Tape, Over Ring and Plexy Glass 10
- 3.6 Four Point Probe Resistance Setup 12

CHAPTER 4: EXPERIMENTAL RESULTS AND DISCUSSIONS 13
- 4.1 Electrodeposition with Single Cathode Terminal Configuration 14
  - 4.1.1 Results and Discussion 17
    - 4.1.1.1 Experiment 1 17
    - 4.1.1.2 Experiment 2 20
    - 4.1.1.3 Study of Surface Roughness 29
- 4.2 Electrodeposition with Double End Cathode Terminal Configuration 34
  - 4.2.1 Results and Discussion 35
    - 4.2.1.1 Performance Characteristics 36
    - 4.2.1.2 Thickness and Conductivity Calculations 37

CHAPTER 5: CONCLUSION 41

CHAPTER 6: FUTURE WORK 42

REFERENCES 43

APPENDIX A: GENERAL INFORMATION ON 3D PRINTING PROCESS….....46

LIST OF TABLES

Table 1 Resistance of Electrodeposited Samples for 795 s.....19

Table 2 Resistance of Electrodeposited Samples at Single Terminal Cathode Configuration.....29

Table 3 Roughness Measurements.....33

Table 4 Resistance Measurements for Two Contact Configurations.....37

Table 5 Thickness Calculations.....39

Table 6 Conductivity Calculations.....40

LIST OF FIGURES

Figure 1 Replicator 2 by MakerBot 3

Figure 2 Conductive PLA Proto-Pasta Spool 4

Figure 3 Electroplating Principle 6

Figure 4 STL File for Insulating Part 10

Figure 5 A) Side View of Assembled Part, B) Top View of Assembled Part 11

Figure 6 A) Plexy Glass Holder Setup, B) Sample With Copper Tape Contacts, C) Top View .. 11

Figure 7 Four Point Probe Setup 12

Figure 8 Keithley Total Resistance Model 13

Figure 9 Dimensions of PLA Strip for Narrow Strip Experiment 14

Figure 10 Single End Cathode Terminal Configuration Connections 15

Figure 11 Code for Current and Resistance Measurement 16

Figure 12 Electrodeposition of Conductive PLA A) at 1.0V, B) at 1.1 V, C) at 1.2 V 17

Figure 13 The Electrodepositing Current vs Time Graph for 1.0 V 18

Figure 14 Electrodeposition Time vs Current at 1.1V 18

Figure 15 Electrodeposited Current vs Time at 1.2 V 19

Figure 16 Electrodeposited Copper on Conductive PLA: A) at 1.0V, B) at 1.1 V, C) at 1.2 V ... 20

Figure 17 SEM Images of Electrodeposited Samples at 1V 21

Figure 18 Electrodeposition Current vs Time at 1V 22

Figure 19 Resistance vs Time at 1V 22

Figure 20 SEM Images of Electrodeposited Sample at 1.1V 24

Figure 21 Electrodeposition Current vs Time at 1.1V 25
Figure 22 Resistance vs Time at 1.1V 25
Figure 23 SEM Images of Electrodeposited Sample at 1.2V 26
Figure 24 Electrodeposition Current vs Time at 1.2V 27
Figure 25 Resistance vs Time at 1.2 V 27
Figure 26 Roughness Measurement at 1V 30
Figure 27 Roughness Measurement at 1.1V 30
Figure 28 Roughness Measurement at 1.2V 31
Figure 29 Thickness of Electrodeposited Sample at 1V 31
Figure 30 Thickness of Electrodeposited Sample at 1.2 V 32
Figure 31 X, Y Directions in Roughness Measurement 33
Figure 32 Experiment Setup for Double End Configuration 34
Figure 33 The Electrodeposited Sample with Two Cathode Terminals at A)1.1V, B)1.2V 35
Figure 34 Electrodeposited Current vs Time at 1.1V 36
Figure 35 Electrodeposited Sample at 1.2V with Two End Cathode Terminal..... 36

ABSTRACT

There are substantial advances in Additive Manufacturing (AM) technologies. The simplest and advantageous technique of AM in terms of cost and scaling of the substrate is Fused Deposition Modeling(FDM). Currently, integration of electronics to a 3D printed structure is done manually after fabrication of the structure. To print electronic circuits directly on a 3D printed structure, copper electroplating process has been studied in this work.

To electroplate on the 3D printed insulating substrate, various materials were studied to make substrate conductive. By using conductive Polylactic Acid (PLA) filaments, a compatible substrate for electroplating was printed. Electroplating was proved to be advantageous in terms of uniform distribution as well as fast deposition rate when performed laterally. The conductive levels of the electrodeposited layers on 3D printed conductive substrates were studied at different voltages in different configurations.

Furthermore, the textures of the electroplated layer were studied using Scanning Electron Microscopy(SEM) method. The resistance of samples was measured using four-point probe resistance setup. The Morphology and roughness of the samples were studied by an optical profilometer system.

In addition, the adhesion strength of the electrodeposited copper on conductive PLA material was tested by a peel test using scotch tape. Thickness and conductivity calculations were performed for uniformly deposited samples. Further study is required for optimizing electroplating process to be used for in situ metallizations of a 3D printed structure.

CHAPTER 1: INTRODUCTION

Technologies that build solid objects from the accumulation and solidification of a material from a computer designed 3D model are represented by a generic name 3D printing or Additive Manufacturing(AM) [1],[2]. In recent times 3D printing technology grabbed an utmost attention to research, industry, consumers which guided the acquisition of significant results in the fields of electronics [3, 4] and structural engineering [5]. Electronics with printed line connections were also being implanted in 3D printed structures. [6, 7].

To integrate electronics with AM, a 3D printer should be able to print a conductive substrate and an insulating substrate. There are few AM techniques to print conductive and insulating materials to realize an electronic prototype, but they have some flaws. Due to high cost, direct energy deposition is not preferred for low-cost prototyping [8]. Because of clogging issue in inkjet printer nozzles, high conductive inks cannot be used [9, 10]. The Selective laser sintering and photopolymerization are two other methods that could not print metals on insulating polymer substrates [11].

On the contrary, a cost-effective machine works with Fused Deposition Modeling (FDM) approach can be bought as a mountable kit with less than $1000 [1]. The Fused Deposition Modeling prints conductive as well as nonconductive materials economically [12]. The conductive polymer used in FDM printer has lower conductivity than the metal. Our work focuses on using electrochemistry in building up a conductive layer on a 3D printed conductive substrate.

CHAPTER 2: BACKGROUND

This chapter presents the basic knowledge of both additive manufacturing and electroplating concepts. The first section focusses on FDM printing and conductive filament used in this work. The second section covers the theory of electroplating process.

2.1 Additive Manufacturing

The 3D printing was first known as Rapid Prototyping based on the initial purpose of prototyping [2]. In later times, the prototype developed from this technology was very near to the real product [2]. The solid objects were directly printed by adding up materials layer by layer [2]. So, the method is known as Additive Manufacturing. Although AM was found in late 1980's, its usage increased from mid (2000-2010) decade [1].

2.1.1 Market Growth in 3D Printing and its Applications

According to Wohler's report 2013, the yearly growth of the global market for AM industry varies from 25 to 30%. It was expected that the market for AM products and services reaches $ 6.5 billion by 2019 [13].

USA has highest AM production systems (38% of all installations across the world). Also, from 30 major companies around the world that manufacture and sell AM equipment, five companies are located in the USA [13].

Electronics market is leading in the global AM market with 21.8% of the whole AM application market. AM applications also boost industrial revolution by some extent due to its 13.4% of applications in the market.

2.1.2 Fused Deposition Modeling

Fused Deposition Modeling is a completely distinctive way to deal with the production of 3D printed objects. In an FDM printer, thermoplastics are heated at the tip of the nozzle just above their melting point and dropped onto a room temperature platform or heated build platform The printed filament cools down and adheres to previously deposited layers to build a hardened 3D object [14],[2].

The 3D printers follow the bottom-up additive fashion to print 3D objects directly from a computer design. The layers are defined by software that takes a progression of advanced cross-areas through a computer-aided design. Depictions of the cuts are then sent to the 3D printer to develop the individual layers [2, 14].

Figure 1, shows a picture of FDM printer (i.e. Makerbot from Replicator 2) that was used in this work. It is a dual extrusion 3D printer. In electronics, a dual extrusion printer enables another level of compatibility by allowing it to print conductive as well as insulating filaments.

The diameter of the nozzle head dictates the printing resolution. The other resolutions seen in recent times were 127 µm and 50 µm [15, 16]. The FDM desktop printer (Makerbot from Replicator 2) used in this work has a resolution of 100µm.

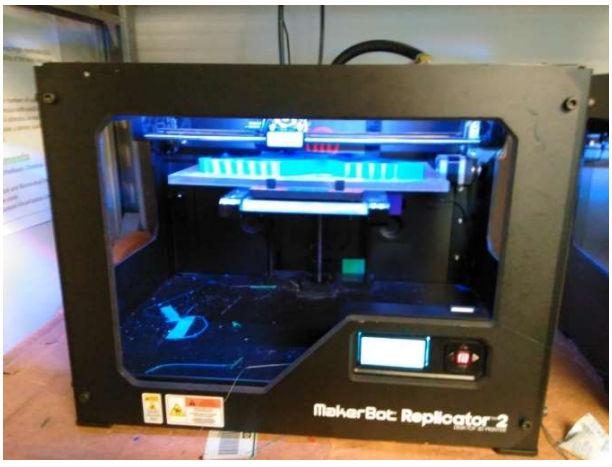

Figure 1 Replicator 2 by MakerBot

An FDM printer has two critical benefits. Firstly, these printers can be effectively adjusted to be incorporated into complex procedures. Secondly, a wide variety of thermoplastics are available as filaments. The latter feature can be used to 3D print conductive or semiconducting polymers, onto plastic structures [1].

2.1.3 Conductive PLA

In our work, a commercially available conductive PLA filament was used for printing a conductive substrate as shown in Figure 2. According to the specifications of the product, the filament has a resistivity of 15 Ω-cm and a diameter of 1.75 mm. It is black in color and is more brittle than the normal PLA. The nozzle diameter ought to be greater than or equal to 4 mm diameter.

Figure 2 Conductive PLA Proto-Pasta Spool

To formulate a conductive filament, carbon fillers are used. A composite with carbon filler becomes conductive when a volume concentration of filler reaches a threshold of about 25% [17]. In choosing a filler ratio, both the percolation threshold and melt viscosity of composite should be considered. The filler ratio must not only be high enough to get a useable electrical conductivity but also must be low enough to allow the material to pass through the heated extrusion nozzle of the 3D printer. Higher loadings of filler lead to a composite that was not able to pass through the standard heated nozzle of a 3D printer [14].

Conductive PLA is not as conductive as metals. As we could not increase the conductivity of polymers beyond a point due to the restriction of filler ratio, electroplating is the best choice to make a conductive PLA substrate more conductive as metals [18].

2.2 Electroplating

Electroplating is an electrochemical process through which the surface of a conductive workpiece can be coated with a layer of a metal, such as copper or silver. This process is also known as electrodeposition. For copper electroplating, the workpiece must be connected to the negative terminal of the power supply (cathode) while the electrode of the coating material is connected to the positive terminal (anode). Here, we used a piece of copper wire as an anode and 3D pattern printed using the conductive PLA material to be coated with copper as a cathode.

In this work of copper electroplating, we used an electrolyte containing an aqueous solution of $CuSO_4$ and H_2SO_4 [19]. The electrolyte is an electric conductor in which current passes through ions but not by free electrons like metals. Electrolyte finishes an electric circuit between two electrodes. When an electric current is applied, the positive ions in the electrolyte will move towards cathode whereas the negatively charged ions move towards the anode. Transfer of ions through the electrolyte constitutes the electric current in that part of the circuit [19].

Electroplating is based on the redox reactions at the anode and cathode electrodes. During the electroplating process metal atoms at the anode, lose electron which is referred as oxidation (Equation-(1)). While on the surface of the cathode electrode, metal ions gain electron which is referred as a reduction (Equation-(2). The rate of cations released from the anode is equal to the rate of the deposition on the cathode.

Electrodeposition is based on two electrochemical reactions as shown in Equations (1) and (2). Oxidation reaction at the anode is given by equation (1).

$$Cu \longrightarrow Cu^{+2} + 2e^{-} \quad (1)$$

Reduction reaction at the cathode is given by equation (2).

$$Cu^{+2} + 2e^{-} \longrightarrow Cu \quad (2)$$

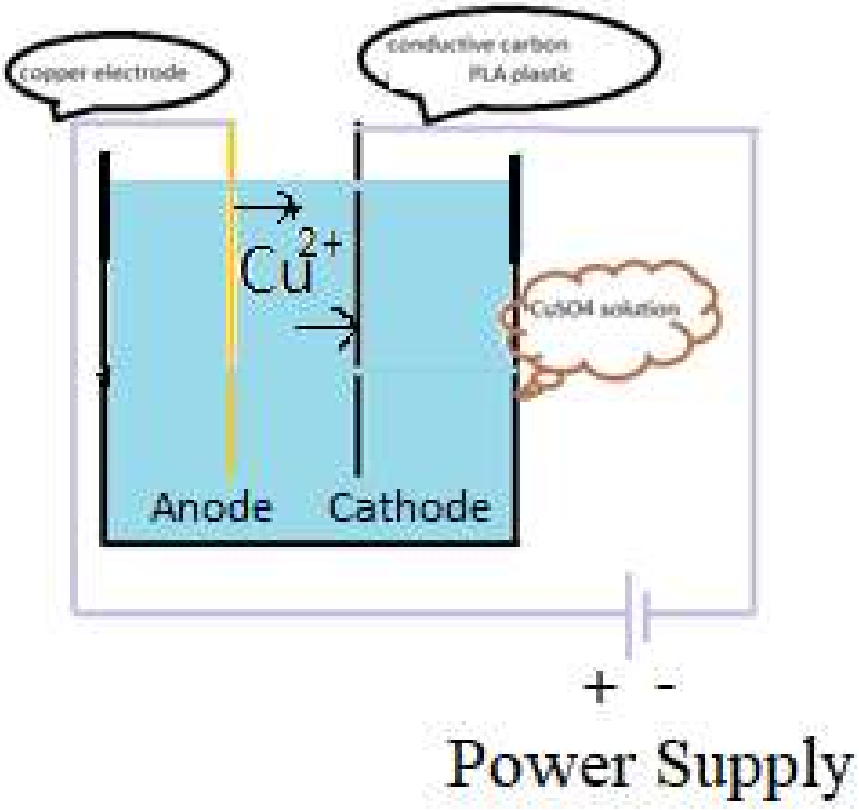

Figure 3 Electroplating Principle

Figure 3 shows a schematic of an electroplating cell with a voltage source connected to the anode and cathode electrodes. The workpiece was provided with negative supply. The electrons from the cathode set the copper ions free and settle as atoms on the cathode surface i.e. conductive workpiece. Simultaneously, the same number of sulfate ions reach the anode, by completing the electric circuit [19]. Anode dissolves gradually and recharges the ions when electrical current flows through the circuit [18].

Current density is the vital factor in electroplating. In this process, current density has an impact on deposition rate, plating adherence, and plating quality which is given by equation (3).

Electroplating deposition rate is directly related to the current density, whereas the adhesion and plating quality are inversely related to the current density [20].

$$\text{current density} = \frac{\text{electroplating current}}{\text{surface area of the workpiece}} \quad (3)$$

Electrodeposition of metal at cathode and dissolution of metal at the anode can occur only if the system is moved away from equilibrium. These electrode reactions can only happen when the external potential is provided. Overpotential is defined as the difference between its equilibrium potential and its operating potential of the electrode potential at the electrode when the current is flowing. The overpotential designates the additional energy required to force the electrode reaction to undergo at a necessary rate. Subsequently, the operating potential of an anode is always more positive than its equilibrium potential. The operating potential of a cathode is always more negative than its equilibrium potential. The overpotential goes up when the current density is increased. The overpotential value also depends on the intrinsic speed of the electrode reaction. A slow reaction which has small exchange current density will need a higher overpotential for a known current density than the fast reaction which has large exchange current density. Overpotential is also referred as the polarization of the electrode. An electrode reaction always happens in more than one basic step, and it has an overpotential related with each step [19].

When small overpotential voltages are applied, there is exponential growth in cathode and anode currents [21]. At higher overpotentials, water electrolysis takes place evolving hydrogen in form of bubbles at the cathode.[22]. During the electroplating process, at the cathode, there is a possibility of occurrence of a reaction mentioned in equation(4) [23].

$$2H^+ + 2e^- \longrightarrow H_2 \quad (4)$$

The absorption of hydrogen occurs in substrate metal as H atoms but not as H_2 molecules [23]. In voids or vacancies, the molecule bubbles may gather [23]. The diffusion of bubbles

towards cathode will help in movement of Cu^{2+} ions through convection and avails the low resistance in the electrolyte, which leads to high current. The growth rate increases substantially due to the formation of copper nanostructures at low density when compared to compact copper [22, 24-26]. In the adsorbed state, hydrogen bubbles cling to the surface which leads to the growth of pores before they are released [23].

CHAPTER 3: EQUIPMENT DESCRIPTION AND MATERIALS PREPARATION

This chapter describes the important equipment and materials used in our work. This chapter also explains the setup clearly.

3.1 Keithley 2602A System Source Meter

Keithley 2602A System source meter is used for all the electroplating experiments. It provides DC supply that is required for electrodeposition. It has two source meter channel, one channel was used for supply voltage and other was used for measuring the resistance of electroplated area when required. In this work "Test Script Builder" software was used to build the test scripts on Keithley test script processor. This software was used to create, manage and run.

3.2 Scanning Electron Microscopy

In SEM, focused beam of high energy electrons generates various signals at the solid sample. The signals which come from electron-sample interactions characterize the morphology. We used "HITACHI S-800 Scanning Electron Microscopy" for the study of morphology.

3.3 Profiling System

We used "Wyko NT 9100 Optical Profiling System" to measure the roughness of electrodeposited copper on the samples printed in this work.

3.4 $CuSO_4$ Solution

The electrolyte was prepared by mixing and stirring 0.75 g of $CuSO_4$ powder and 1.5 g of H_2SO_4 in 10 ml of de-ionized (DI) water using a small magnet which results in 0.40 M $CuSO_4$ in 1.32 M H_2SO_4.

3.5 Copper Wire, Copper Tape, Over Ring and Plexy Glass

For the electroplating, a piece of copper wire was used as the anode in this work. Copper tape was used for making contacts between the Keithley probes and the sample.

Using a conductive PLA filament, it is possible to print a conductive "template" pattern to be the cathode electrode for copper electroplating. However, due to the high resistivity of the printed electrode, the potential difference across the cathode could be significant. This affects the deposition rate to be different at different spots. To make the deposition more uniform, lateral electrodeposition was used in this work.

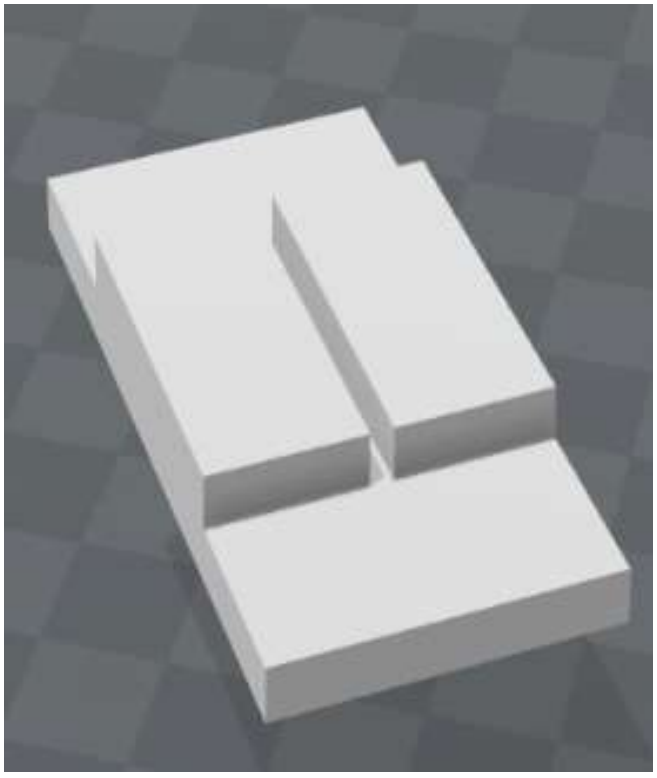

Figure 4 STL File for Insulating Part

As this work is inclined to FDM printing, extremely profound assembled part was designed which constitute conductive PLA and normal PLA as shown in Figure 4. The part file of the normal PLA is shown in Figure 4. The conductive PLA strip was designed with dimensions corresponding to the configuration used in chapter 4 to exactly fit into the base of the insulating substrate.

Furthermore, the assembly files were designed from the individual part files in a computer-aided software SOLIDWORKS. Figure 5 depicts the side view in which black part on top was made of conductive PLA and white part that hold black strip was made of an insulating PLA

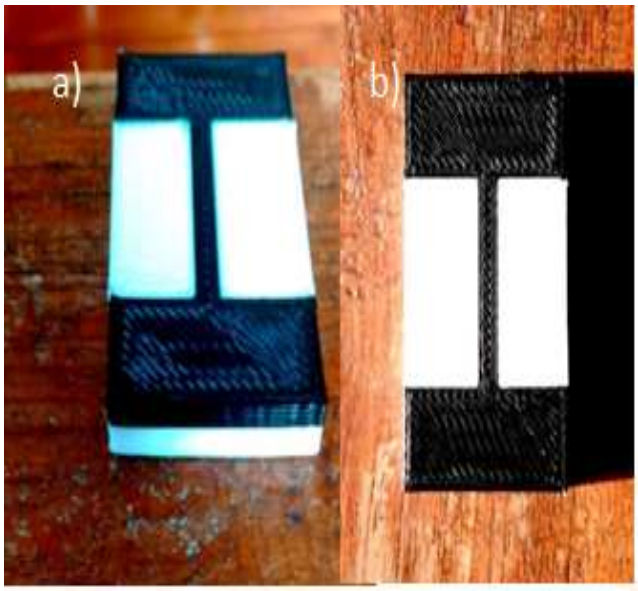

Figure 5 A) Side View of Assembled Part, B) Top View of Assembled Part

Figure 6, shows the setup that was used for making a small electroplating bath over the sample. From Figure 6(a), two rectangular plexiglass pieces with a circular opening of 15 mm diameter at the center provide contact to the copper metal piece (anode) in the electrolyte.

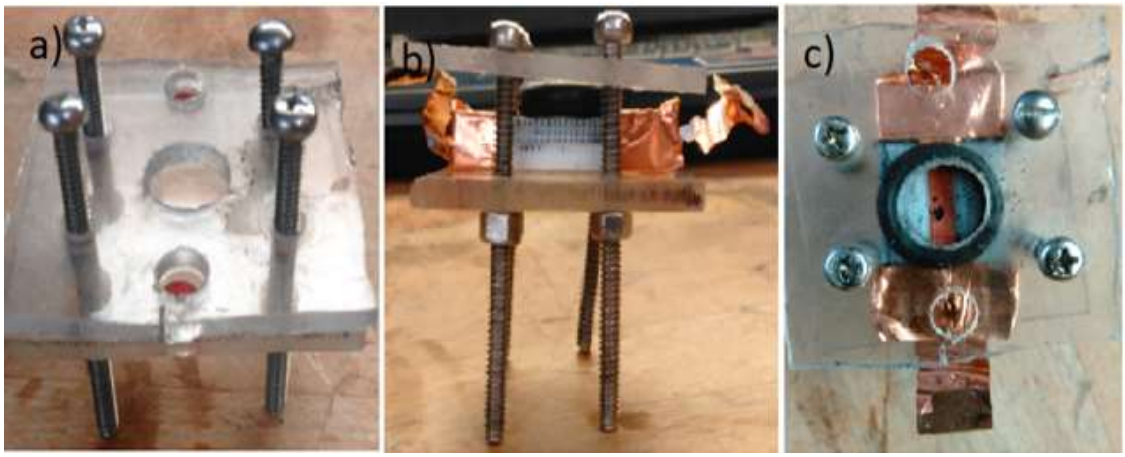

Figure 6 A) Plexy Glass Holder Setup, B) Sample with Copper Tape Contacts, C) Top View

The copper tape strengthens the contact between the source voltage probe (Channel A from KEITHLEY) and substrate as shown in Figure 6(b). It is easy and economical to make a contact with the copper tape.

In addition, two holes on either side of top plexiglass avail a mechanical support for the alligator to make a reliable contact with copper tape on the sample as shown in Figure 6(c).

Moreover, the over ring on top of the substrate was fixed in between plexiglasses with the tightened nut and bolt on its four corners, so that it could hold the electrolyte without any leakage. In this work, the anode is placed in the electrolyte without contacting the cathode (black colored conductive PLA). This completes the whole setup to conduct a lateral electroplating experiment on a 3D printed sample.

3.6 Four Point Probe Resistance Setup

This set up is used to measure the resistance of the sample by passing current through two outer probes whereas voltage is measured across two inner probes as shown in Figure 7.

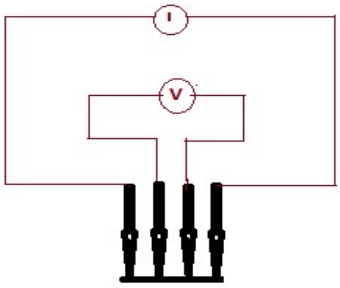

Figure 7 Four Point Probe Setup

CHAPTER 4: EXPERIMENTAL RESULTS AND DISCUSSIONS

This chapter presents the results obtained from the two experiments. The first experiment was conducted on a track with its width equal to 2.25 mm. Electroplating currents were recorded during the experiment for further analysis. The second experiment was focused on increasing the electroplating quality on the track. The electrodeposition process in this work depends on the following factors.

- The conductivity of the printed black strip.
- Contact between the source and the substrate.

The results obtained from the Keithley were not the exact resistance values for the electroplated area. The resistance measured by the Keithley 2602A source meter includes the resistance of the copper tape on either side which was denoted as R_{c1} and R_{c2} as shown in Figure 8. It also includes the resistance of uncoated conductive PLA on either side which was denoted as R_{p1} and R_{p2} as shown in Figure 8. Total resistance measured by Keithley was denoted as R_K.

- $R_K=R_{c1}+R_{p1}+R_{p2}+R_{c2}+R_{\text{electrodeposited PLA}}$

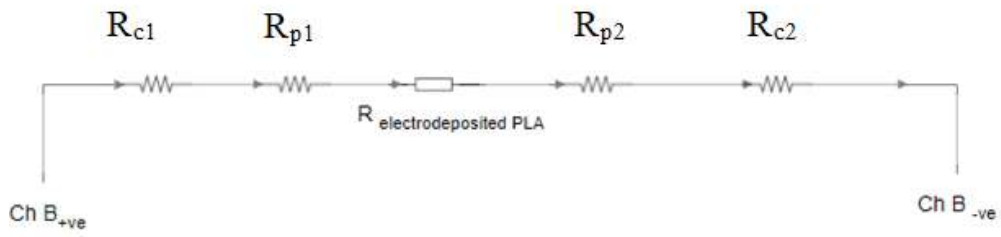

Figure 8 Keithley Total Resistance Model

The resistance of the electrodeposited portion i.e. $R_{eletrodeposited\ PLA}$ was required for analyzing the conductivity of the electrodeposition. The exact resistance across the electrodeposited edges was measured by four-point probe resistance setup for all samples.

The voltage across the substrate that lies in the electrolyte was not equal to the voltage applied to a sample because of the voltage drop across the copper contacts and uncoated black colored conductive PLA on cathode terminal as shown in Figure 8. The actual voltage across the conductive PLA substrate is the different voltage after excluding drop across contacts and uncoated PLA.

4.1 Electrodeposition with Single Cathode Terminal Configuration

The conductive strip in between the substrate was designed with 2.25mm as shown in Figure 9.

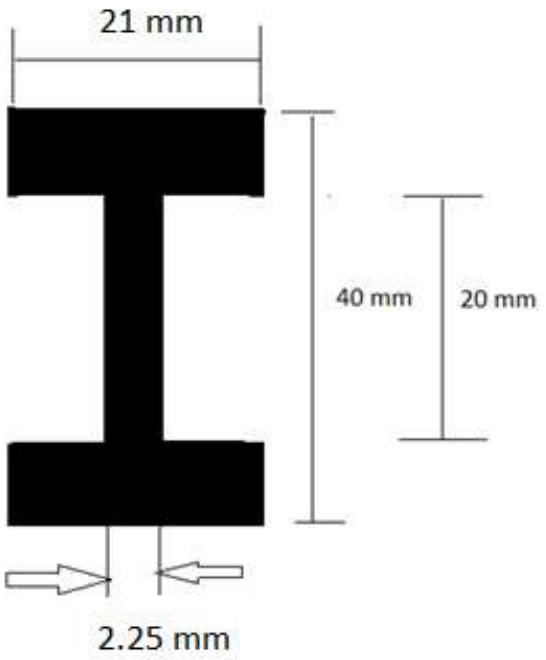

Figure 9 Dimensions of PLA Strip for Narrow Strip Experiment

The connections were given as shown in Figure 10. In this experiment, channel A was used as a source for the electrodeposition process. The positive terminal of the channel A was connected

to the copper piece i.e. anode of the electrodeposition process. The negative terminal of channel A was connected to the copper tape on the conductive PLA i.e. cathode of the electrodeposition process. Channel B was connected across the sample to measure the resistance across it.

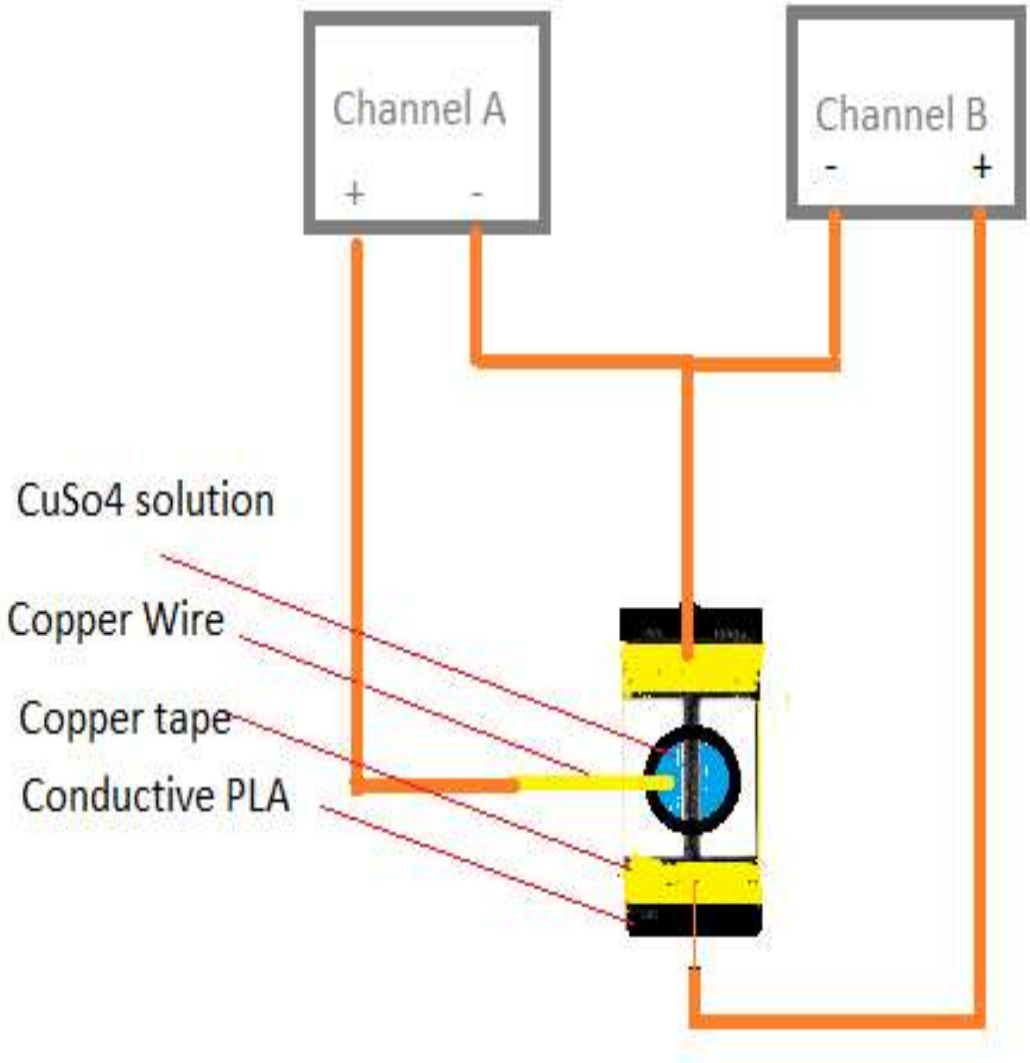

Figure 10 Single End Cathode Terminal Configuration Connections.

The data points for the current and resistance values were found with the Keithley 24602A source meter. To simultaneously collect the data during electrodeposition process, Test Script builder used a programming code such that it measures 200 current values from Channel A and 10 resistance values from Channel B and loops back to measure current and resistance readings

repetitively as shown in Figure 11. It was set such that beep sound comes at the beginning and the ending of the experiment.

```
ON = 1
OFF = 0

beeper.beep(1,500)
smua.reset()
smub.reset()
smub.source.output = OFF

--TODO turn autozero off later
for j=1, 220 ,1 do
smua.source.output = ON

for i = 1, 200, 1 do
    smua.source.levelv = 1.2
    reading = smua.measure.i()
    print(reading)
end
smua.source.output = OFF
smub.source.output = ON
for k = 1, 10, 1 do
    smub.source.levelv = 0.1
    reading1 = smub.measure.i()
    reading=0.1/reading1
    print( "Ri" .. reading)
end
smub.source.output = OFF


end
beeper.beep(1,500)
--if reading < 10 then print("pass")end


smua.source.output = OFF
```

Figure 11 Code for Current and Resistance Measurement

All the data points obtained using Keithley 2602A source meter were used to plot with time. The code shown in Figure 11 runs for 13min and 15s corresponding to the i, j, k values in it.

The code can be altered to run it for the required amount of time. All the data points corresponding to current and resistance values were considered with equal time intervals, this was one of the approximation to get a plot for current vs time and resistance vs time. The time interval between the data points was calculated to be 17.20 ms.

4.1.1 Results and Discussion

Initially, the electrodeposition was conducted for 13 minutes 15 seconds at 1.0V, 1.2V, 2.0V. In this configuration, only single end of the sample was connected to the cathode. The same experiment was repeated in the same configuration for a longer duration to study morphology and other characteristics.

4.1.1.1 Experiment 1

The electrodeposition layer at the different voltages was observed as shown in Figure 12. There was a poor coverage of copper deposition at 1.0 V and 1.1V whereas, at 1.2 V, the copper was deposited completely along the black conductive PLA strip.

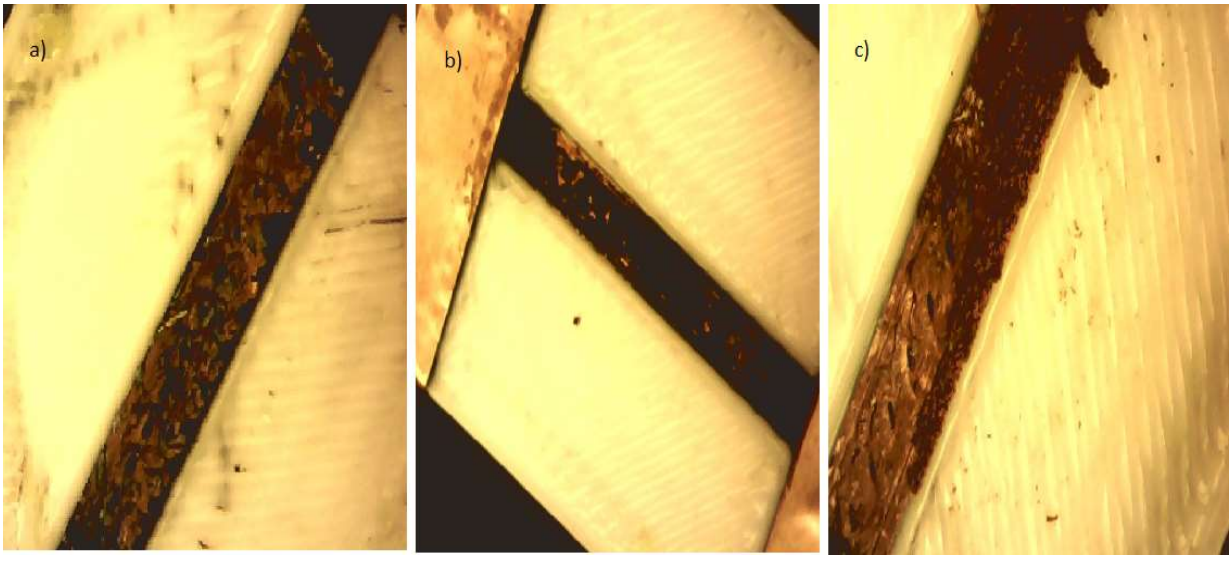

Figure 12 Electrodeposition of Conductive PLA A) at 1.0V, B) at 1.1 V, C) at 1.2 V

The current at 1.0 V was constant throughout the electrodeposition process as shown in Figure 13. The average current was found to be 2.1 mA approximately.

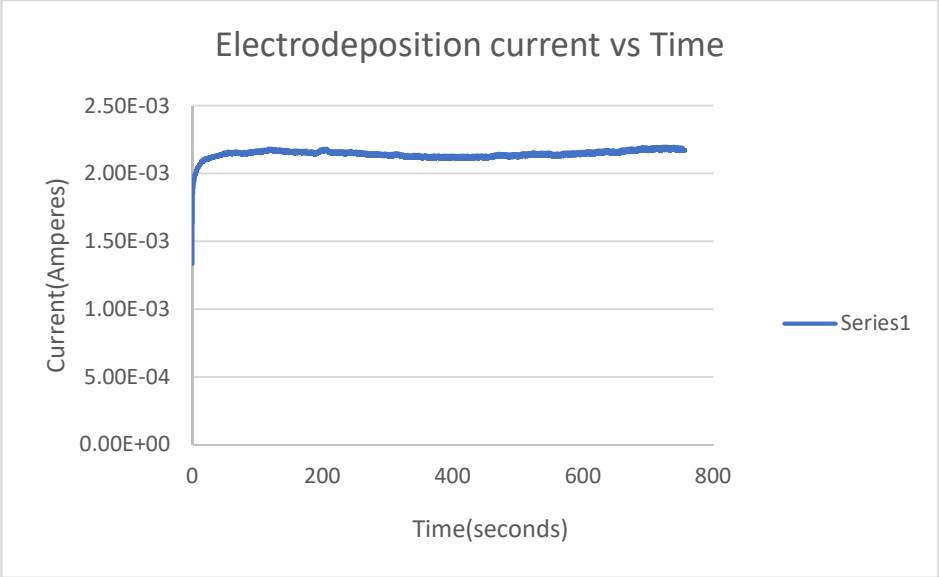

Figure 13 The Electrodepositing Current Vs Time Graph for 1.0 V

Apart from the sudden rise in current, the current was constant during electrodeposition at 1.1V as shown in Figure 14. The average current was observed to be 2.3 mA as shown in Figure 14.

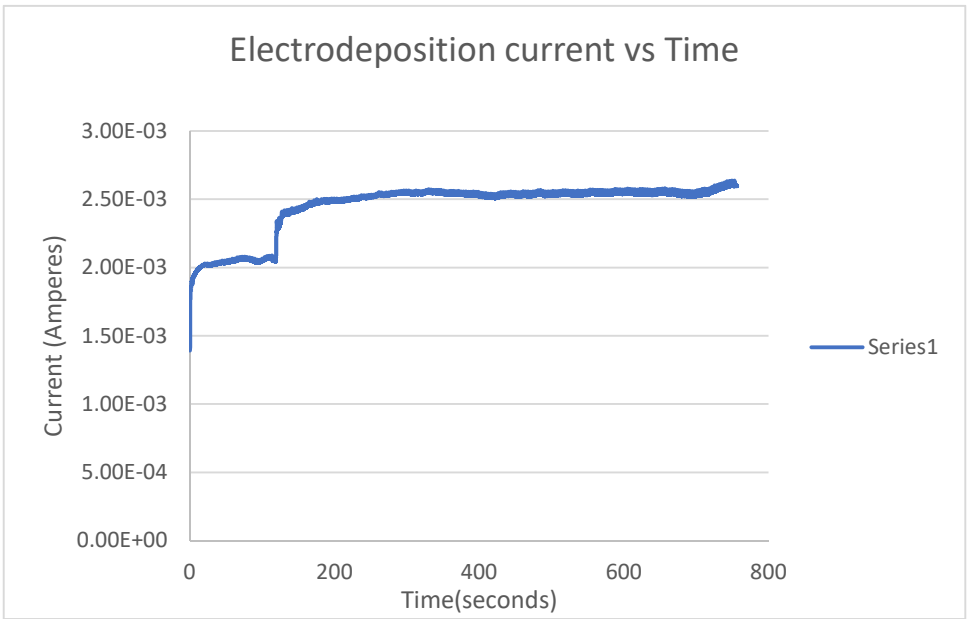

Figure 14 Electrodeposition Time vs Current at 1.1V

The currents at 1.2V were varying as shown in Figure 15. There were bubbles observed during the electrodeposition current swings. This phenomenon was analyzed with the SEM images in next section.

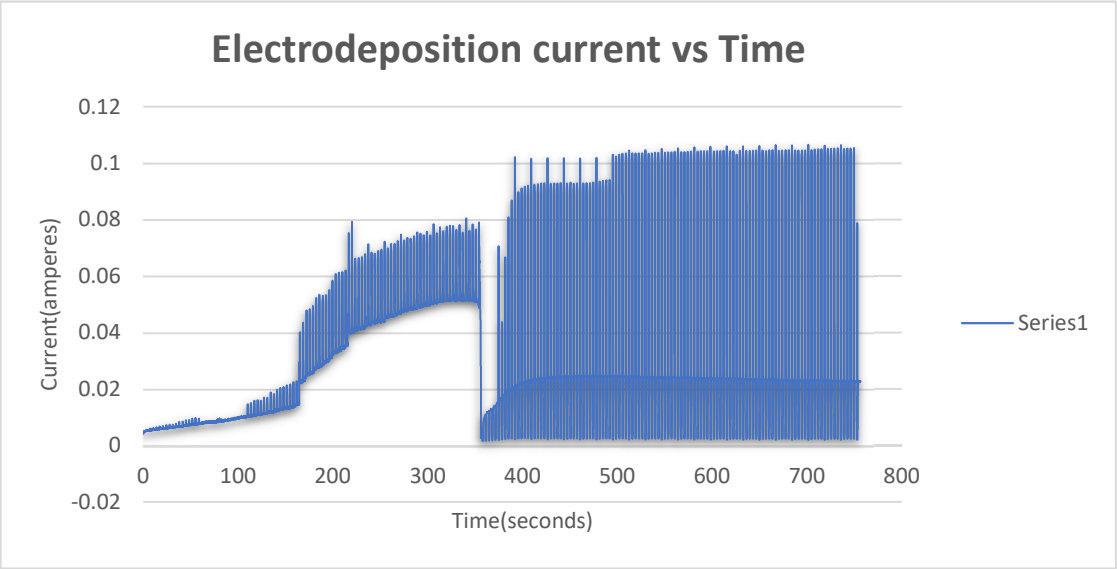

Figure 15 Electrodeposited Current vs Time at 1.2 V

The resistances of the electroplated samples were tabulated as shown in Table 1.

Table 1 Resistance of Electrodeposited Samples for 795 s

Electroplating Voltages(V)	Resistance by four-point probe measurement setup
1.0	20Ω
1.1	5 Ω
1.2	800 m Ω

4.1.1.2 Experiment 2

To study the morphology and the roughness of the electroplated layer, electroplating was extended to longer times to get the good amount of deposition.

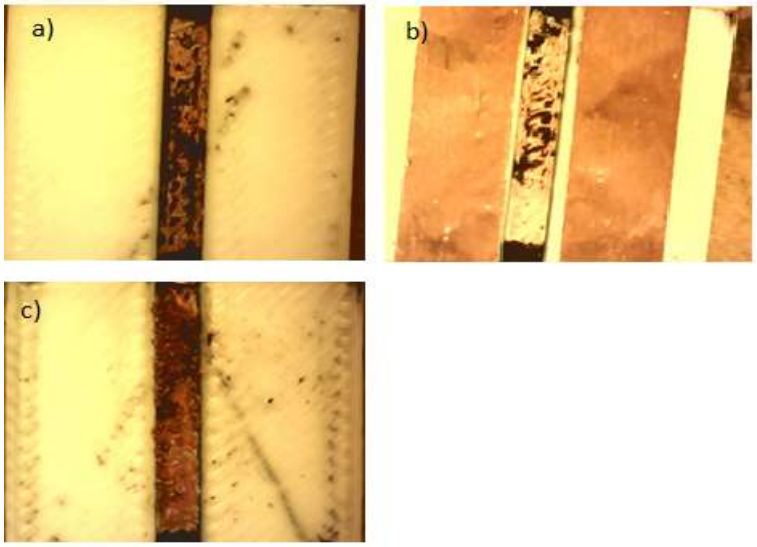

Figure 16 Electrodeposited Copper on Conductive PLA: A) at 1.0V, B) at 1.1 V, C) at 1.2 V

Electroplating at 1.0V was conducted longer due to poor deposition rate, although the electrodeposited area had few spots uncoated. The electrodeposition was started at the cathode terminal of the conductive PLA strip. It was observed that the copper deposition was decreasing from cathode connected end (i.e. top of the sample in Figure 16a) to another end(i.e. bottom of the sample in Figure 16a). At 1.1V, copper deposition had been following the same pattern of decreased coverage along the conductive PLA strip from cathode end terminal to another end (from. bottom to the top of the sample) as shown in Figure 16.b.

At 1.2V the substrate was found with an unusual structure. It was growing very fast after 13min and 15s (i.e. 795 s). There were many bubbles in the electrolyte. Moreover, a very rough surface was observed at the cathode end of the substrate as shown in the top of Figure 16c.

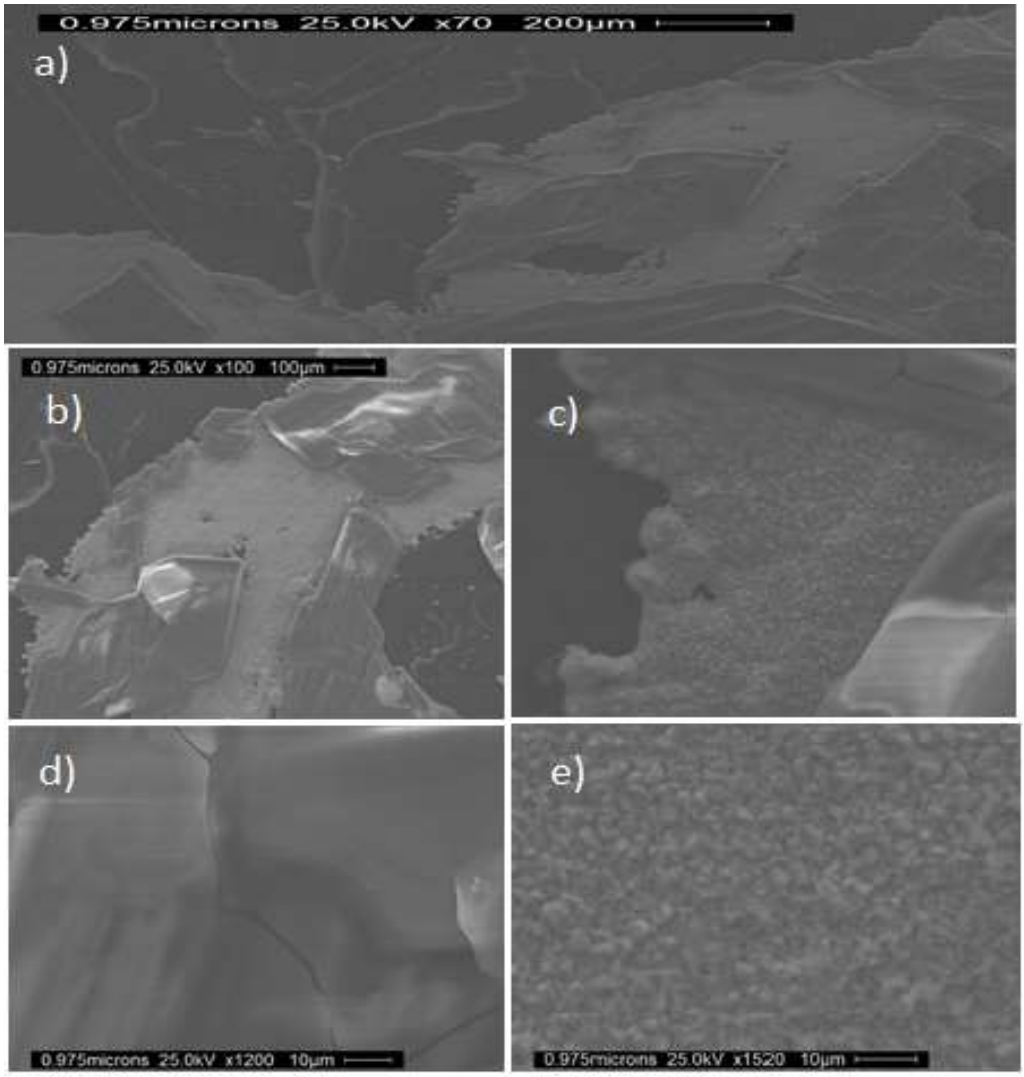

Figure 17 SEM Images of Electrodeposited Samples at 1V

At 1.0 V electrodeposition was conducted for 2,385 seconds. The conductive PLA and the deposited copper can be observed on the top left corner of Figure 17a and on the bottom right corner of Figure 17a respectively. It can be observed that the copper deposited did not follow the same morphology as the substrate. There were two kinds of morphologies as shown in Figure 17 c, d, e, one is a rough surface with a grain structure as shown in Figure 17e whereas another morphology depicts a very smooth surface as shown in Figure 17d. The electrodeposition current and resistance data points were plotted against the time.

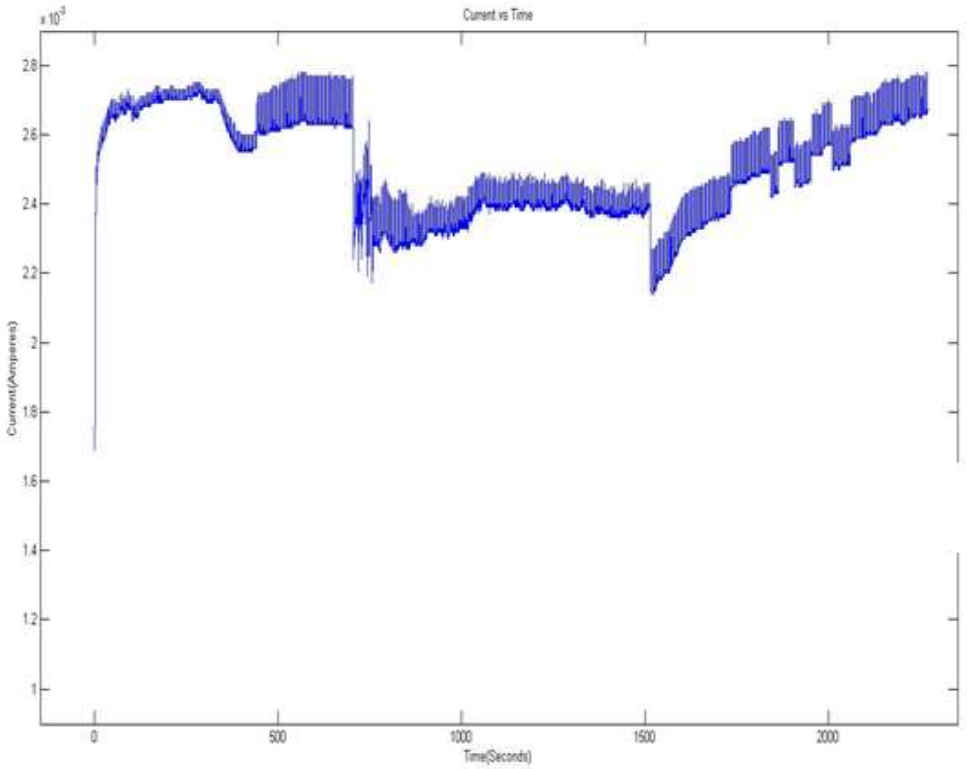

Figure 18 Electrodeposition Current vs Time at 1V

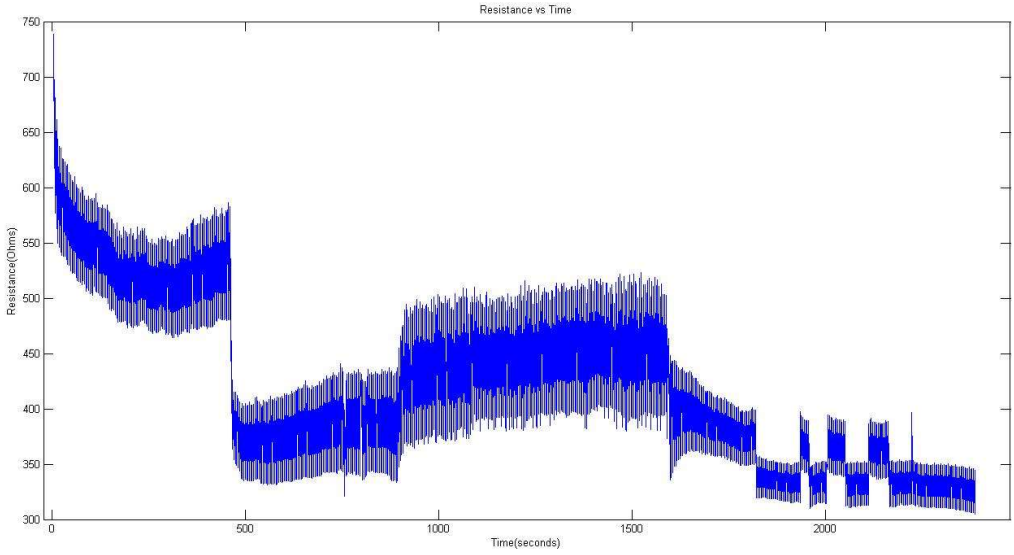

Figure 19 Resistance vs Time at 1V

From Figure 18, it can be stated that the electrodeposition current had increased from 1.7 mA to 2.6 mA just after the copper deposition was started over the substrate. The resistance of this sample had decreased gradually till 500s due to increase in electrodeposition current. Current increased sharply at 500s due to which there was a sudden drop in resistance. The current was fluctuating constantly till the 1800s approximately. As the electrodeposition current had risen suddenly just after the 1800s, the resistance had dropped again. The sudden increment in electroplating currents due to varied overpotentials, the current density also rises with time (as shown in Figure 18). Because of changing current densities, morphologies also vary on electrodeposited layer [18, 25].

The swinging of current very frequently at a consistent band was due to the resistance measurement. Channel B of the source meter was connected across the sample to measure resistance. As seen in Figure 11, 0.1V was applied across sample and resistance was measured by Keithley from corresponding currents across it after every 200 data points of electrodeposition current from channel A to get 10 resistance values from channel B. The electrodeposition current drops due to the measurement of resistance across the sample.

At 1.1 V morphology and performance characteristics were studied as follows. Electrodeposition at 1.1V was done for 1590 seconds. The morphology observed in SEM images at 1.1V (as shown in Figure 20) was uniform. We could see few cracks in the electrodeposited substrate at 1.1V as shown in Figure 20e. The crack width was found to be 0.975 microns as shown in Figure 20e. These cracks might have occurred due to the rough surface of the sample. The coverage of electrodeposited sample at 1.1V was more than the sample electrodeposited at 1.0 V.

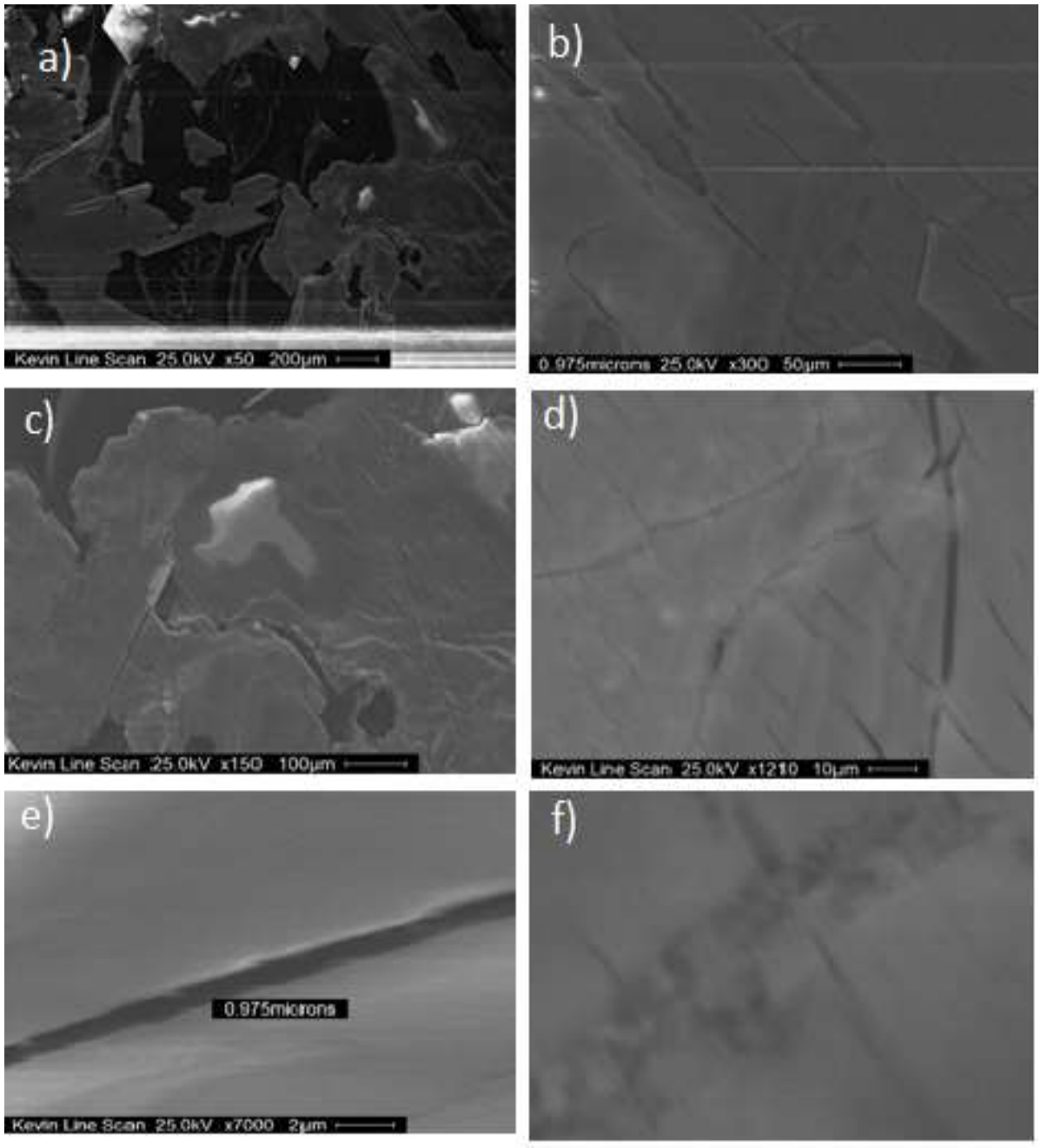

Figure 20 SEM Images of Electrodeposited Sample at 1.1V

The electrodeposition current and resistance data points were plotted against the time. When the electrodeposition was conducted at 1.1V, the electrodeposition current had risen from 2.4mA to 3.3mA (as shown in Figure 21) just after the electrodeposition had started. The average current at 1.1V was higher when compared to currents at 1.0V. Due to the greater deposition rate

at 1.1V, the electrodeposition was performed for 26min 30s, i.e.1590s, which was less than the deposition time at 1.0V.

There were changes in the current without sudden jerks. As there was no sudden rise in current, the current density also remained almost constant due to constant overpotentials which in turn leads to a uniform morphology of the sample.

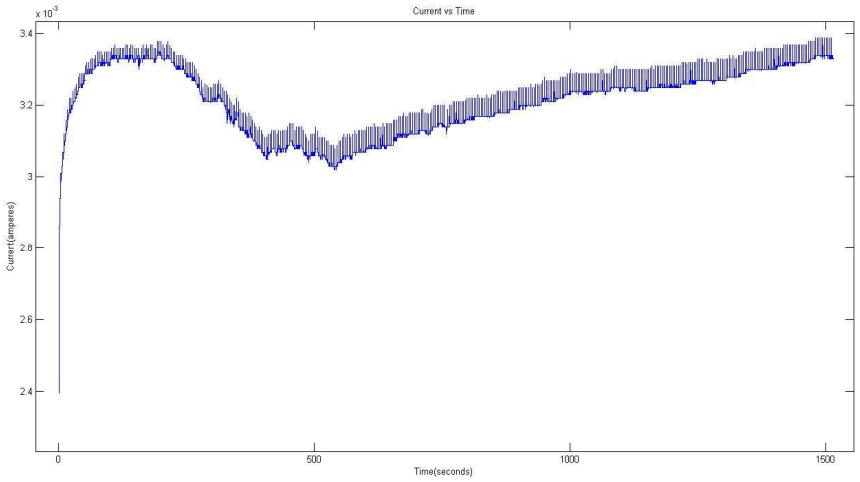

Figure 21 Electrodeposition Current vs Time at 1.1V

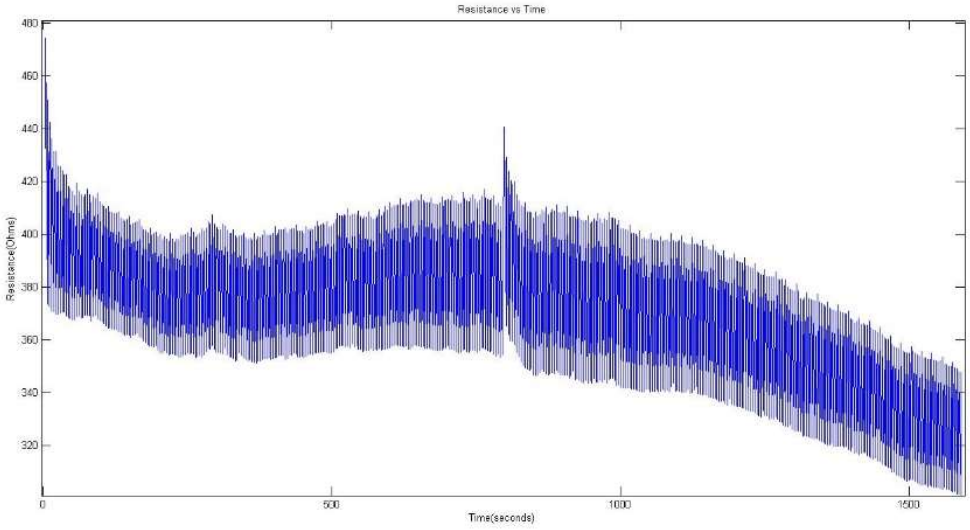

Figure 22 Resistance vs Time at 1.1V

The study of morphology and performance characteristics at 1.2 V was discussed below. The Roughness difference between the conductive PLA (as shown in Figure 23a) and the electrodeposited copper (as shown in Figure 23b) can be observed from the corresponding figures.

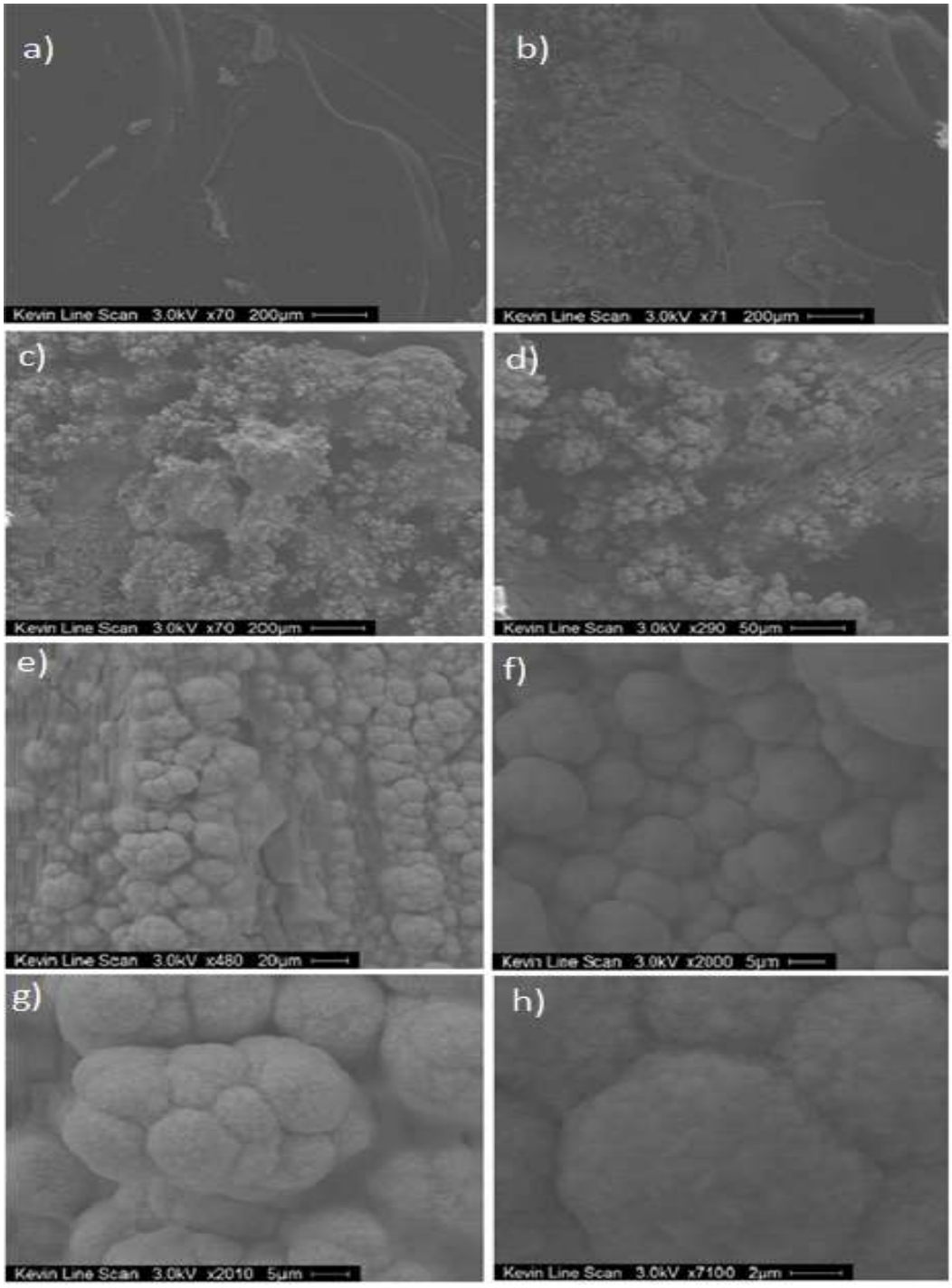

Figure 23 SEM Images of Electrodeposited Sample at 1.2V

When the SEM images of electrodeposited samples at 1.0V and 1.1V as shown in Figure 17 and Figure 20 were compared with SEM images of the electrodeposited sample at 1.2V as shown in Figure 23, a different kind of morphology was observed during copper deposition at 1.2V. The morphology was porous and disperse and was observed from Figure 23 c, d, e, f. The shape and size of copper grains can be observed from Figure 23g and h. It was because of evolved hydrogen at higher overpotential [22].

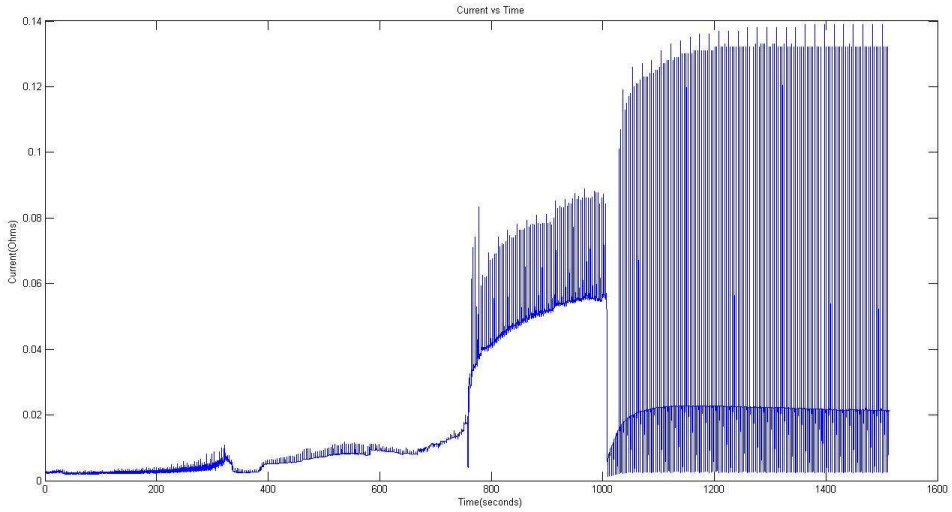

Figure 24 Electrodeposition Current vs Time at 1.2V

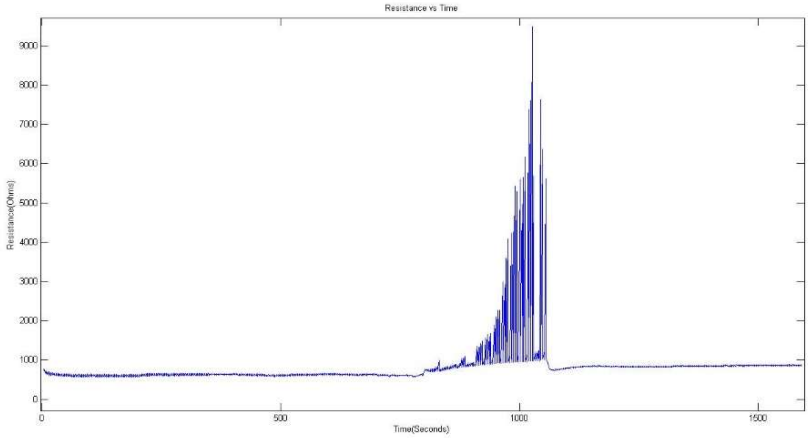

Figure 25 Resistance vs Time at 1.2 V

Suddenly, very high swinging currents were observed just before 800s and continued the same pattern till 1000s as shown in Figure 24.

After 1000 seconds, electrodeposition current remained very low for approximately 25s, where resistance increased to a very high value around 5kΩ. This phenomenon of very high resistance was due to the instance where bubbles bulge out before bursting. This bulging continued for approximately 25s. Due to this expanded bubble, the current decreased to very low value and increased rapidly after it was burst.

After the bubble was burst, very high currents were observed in between the band of low currents. These high currents had occurred due to the repeated process of bulging and bursting of hydrogen bubbles. This trend was followed from 1200 to 1500 seconds.

As the currents had been swinging very rapidly, the current density also had changed very rapidly. Due to the rapid change in current density, the morphology of deposition had been non-uniform through the electrodeposited surface[25]. Hydrogen evolution phenomenon results with a very rough surface on the substrate [23].

The resistance of the electroplated samples at different voltages was measured by a four-point probe resistance setup and was tabulated in Table 2. As adhesion was also an important criterion for electrodeposited copper, the peel test was conducted to check the adhesion capacity of the electrodeposited sample. An adhesion test was done in a simple way with the help of Scotch tape. We used a 3mm wide scotch tape to put on the electrodeposited spot of the sample. The Scotch tape was ripped off and resistance was found with four-point probe resistance measurement. The difference between the resistance before and after the peel test demonstrates the adhesion strength of the electrodeposited copper.

Table 2 Resistance of Electrodeposited Samples at Single Terminal Cathode Configuration

Sample type	Electroplating time(s)	Resistance	Resistance Observed after peel test
Bare sample	0	152.2 Ω	152.2 Ω
Electrodeposited copper strip at 1V	2,385	45mΩ	75mΩ
Electrodeposited copper strip at 1.1 V	1,590	60 mΩ	100mΩ
Electrodeposited copper strip at 1.2 V	1,590	65 mΩ	170mΩ

4.1.1.3 Study of Surface Roughness

The surface roughness was found by Wyko nt 9100 profilometer. As the arithmetic average of roughness profile has been widely used, R_a was used to represent the roughness in this work.

Although the electrodeposition was performed at 1V for very long time (2385 s), the electrodeposition had a poor coverage resulting in few patches deposited. The roughness and thickness were high as shown in Figure 26. At 1.1V the electrodeposition current density was uniform. This results in less roughness compared to the electrodeposited sample surface at 1V as shown in Figure 27.

The step height was not found on the electrodeposited sample at 1.1 V as the roughness of the deposited copper and the bare sample was same.

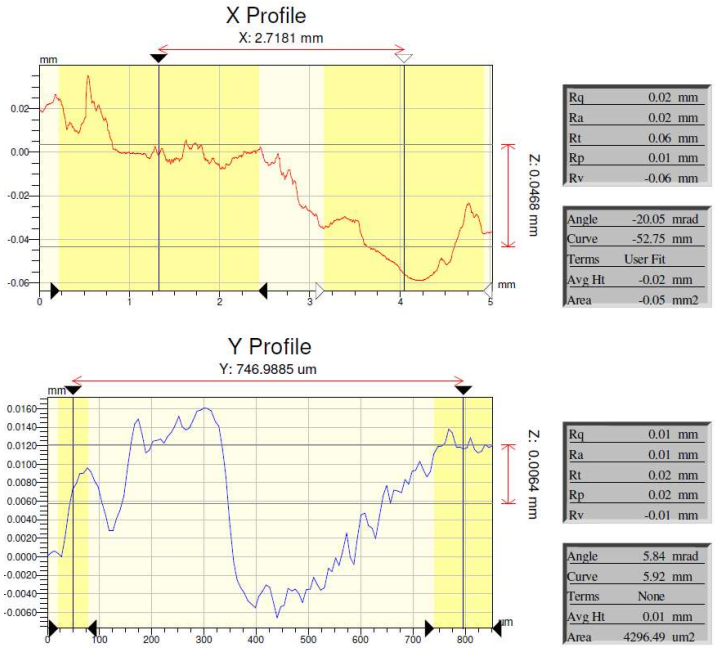

Figure 26 Roughness Measurement at 1V

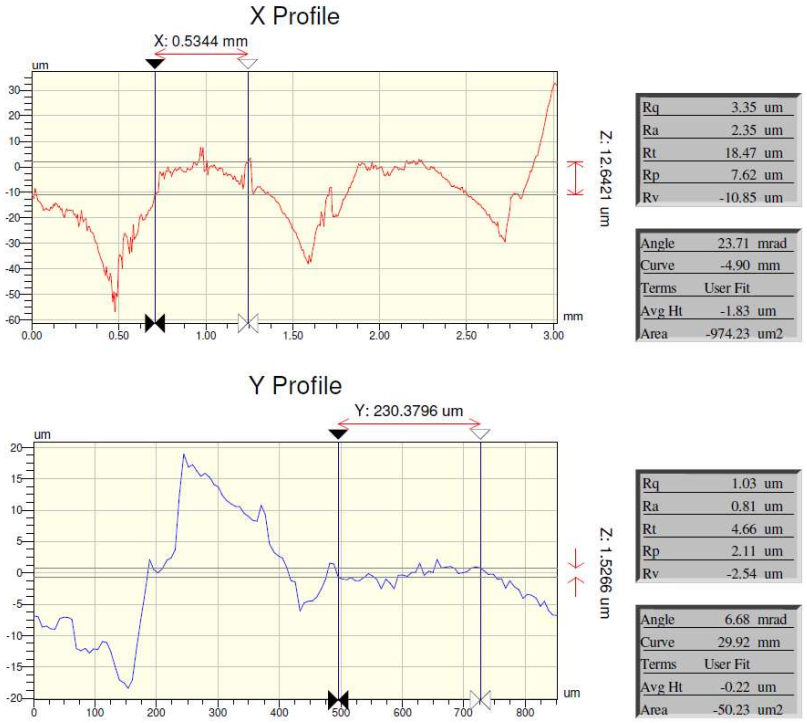

Figure 27 Roughness Measurement at 1.1V

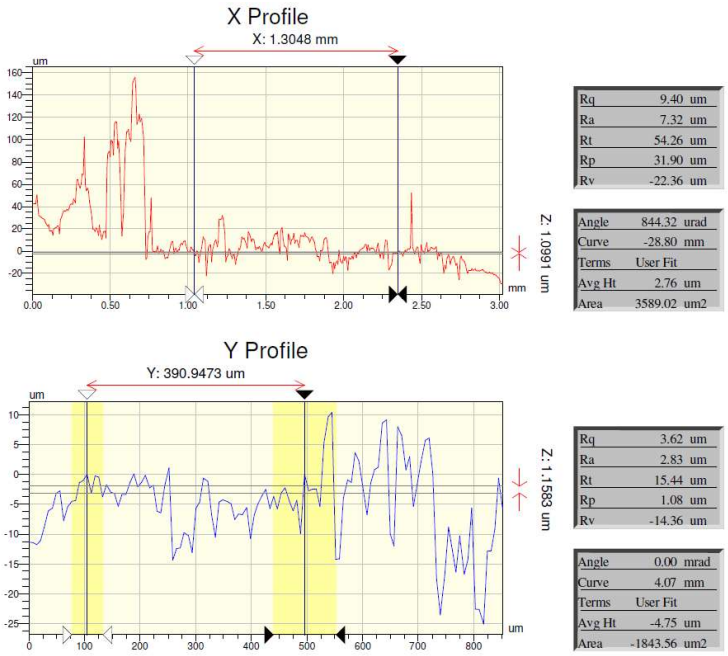

Figure 28 Roughness Measurement at 1.2V

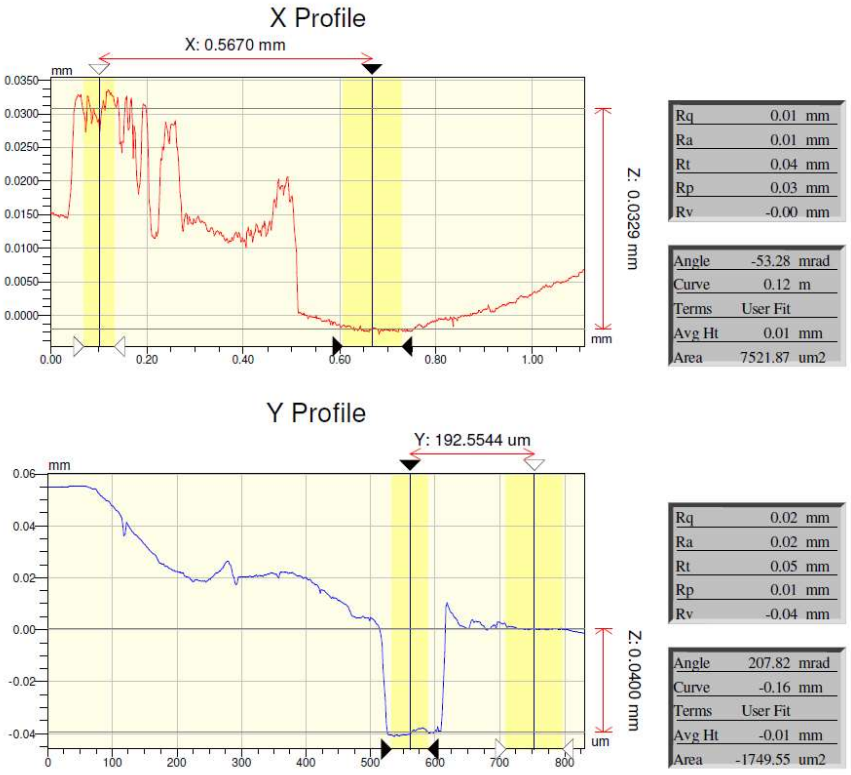

Figure 29 Thickness of Electrodeposited Sample at 1V

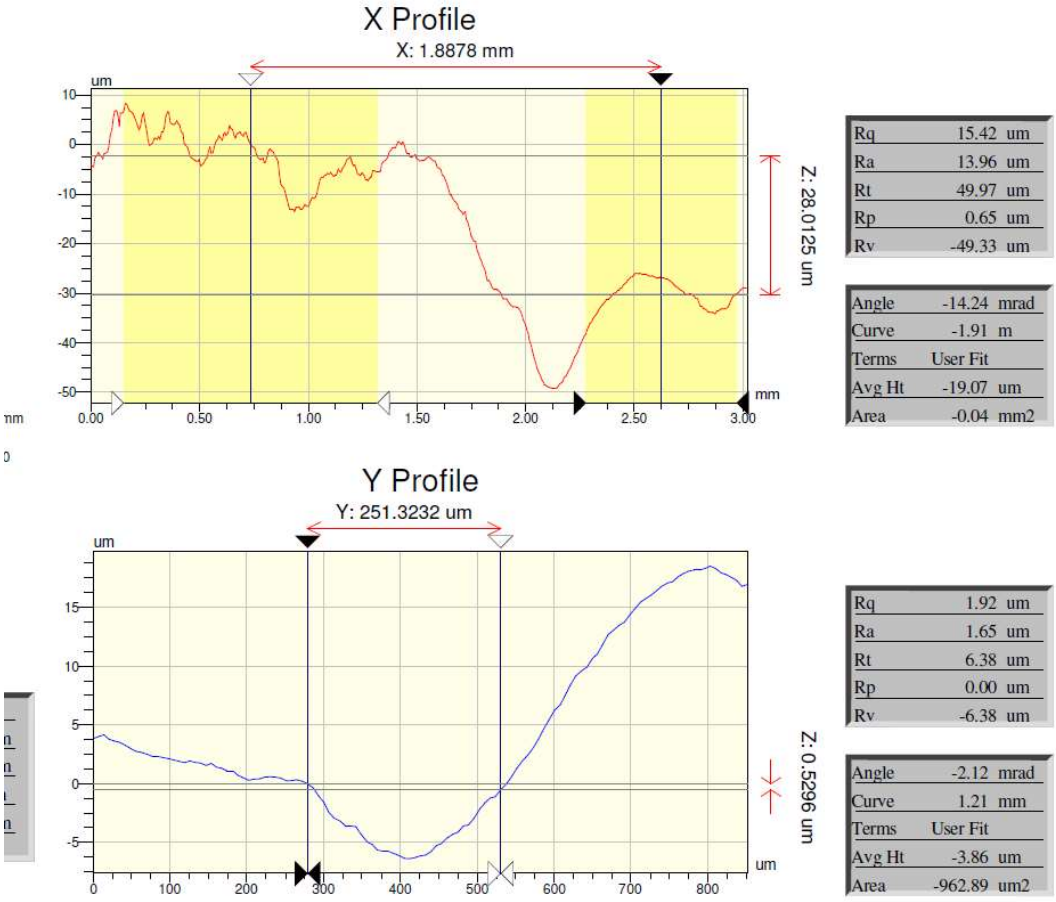

Figure 30 Thickness of Electrodeposited Sample at 1.2 V

At 1.2V the surface roughness was higher at the spot where hydrogen evolution took place, roughness was measured at the point where roughness seems low. The minimum roughness of the copper deposited at 1.2V was observed to be greater than the roughness observed at 1.1V. This follows the trend of increasing roughness with increased electroplating voltages [27].

The roughness measured for different voltages were tabulated in Table 3. The thickness of the electrodeposited samples was calculated from the roughness measurements done at the point where the electrodeposition had started.

The thickness of the electrodeposition was calculated from the average roughness difference at either side of the junction where electrodeposition started. This calculation was done based on the x- profile measurement, as the junction lies along the x-direction. From 1.0V

measurements as shown in Figure 30. The average roughness difference was calculated to be 14.5 µm along the x-direction. The average roughness difference at 1.2 V as shown in Figure 31 was calculated to be 26 µm.

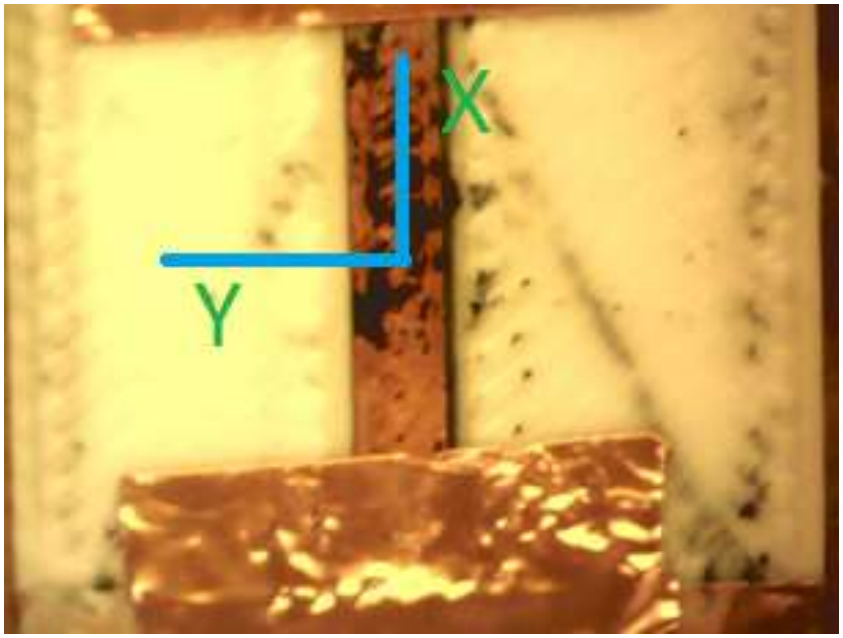

Figure 31 X, Y Directions in Roughness Measurement

Table 3 Roughness Measurements

voltage	R_a for X direction (µm)	R_a for Y-direction (µm)
1V (5 mmx0.84 mm)	20	10
1.1V (3mmx0.84 mm)	2.35	0.81
1.2V (3 mmx0.84 mm)	7.32	2.83

4.2 Electrodeposition with Double End Cathode Terminal Configuration

As the sample was printed in lines the printed plastic deposited hardened immediately. A rough surface with peaks and valleys were created in FDM printing process[15].This experiment's main aim was to find out the best method for uniform electrodeposition on the rougher surface area. As our work was focused to develop a conductive track as an alternative to PCB by a 3D printing method. We have been working for a reliable deposition on the narrow track.

Electroplating was conducted for two voltages on similar samples with a small ring at center with 1.5 cm diameter containing the CuSo4 electrolyte. The scheme of connection was changed in this experiment as shown in Figure 33.

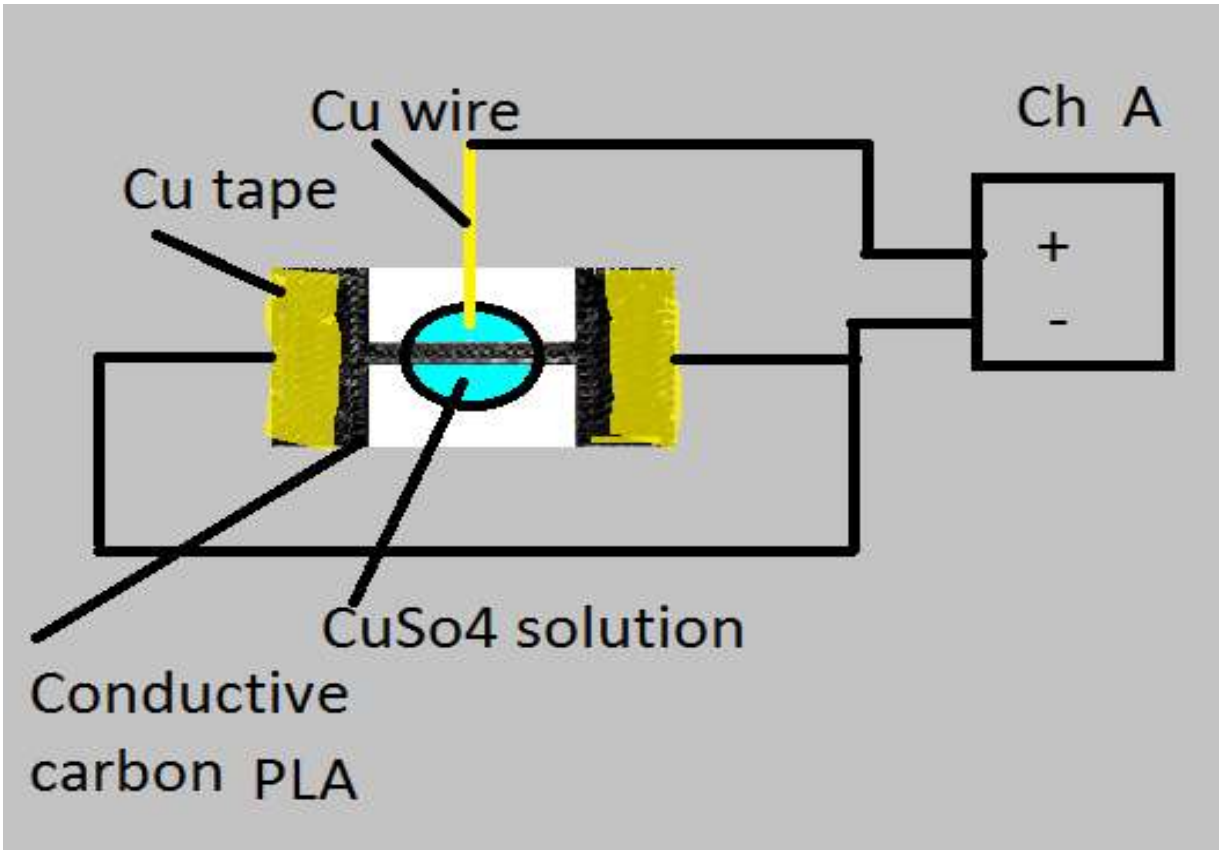

Figure 32 Experiment Setup for Double End Configuration

The positive terminal of Channel A was connected to the copper wire (anode) and the negative terminal was connected to both ends of the sample. As two ends of the sample were shorted, resistance measurement could not be done with the current apparatus (Keithley) in this experiment.

4.2.1 Results and Discussion

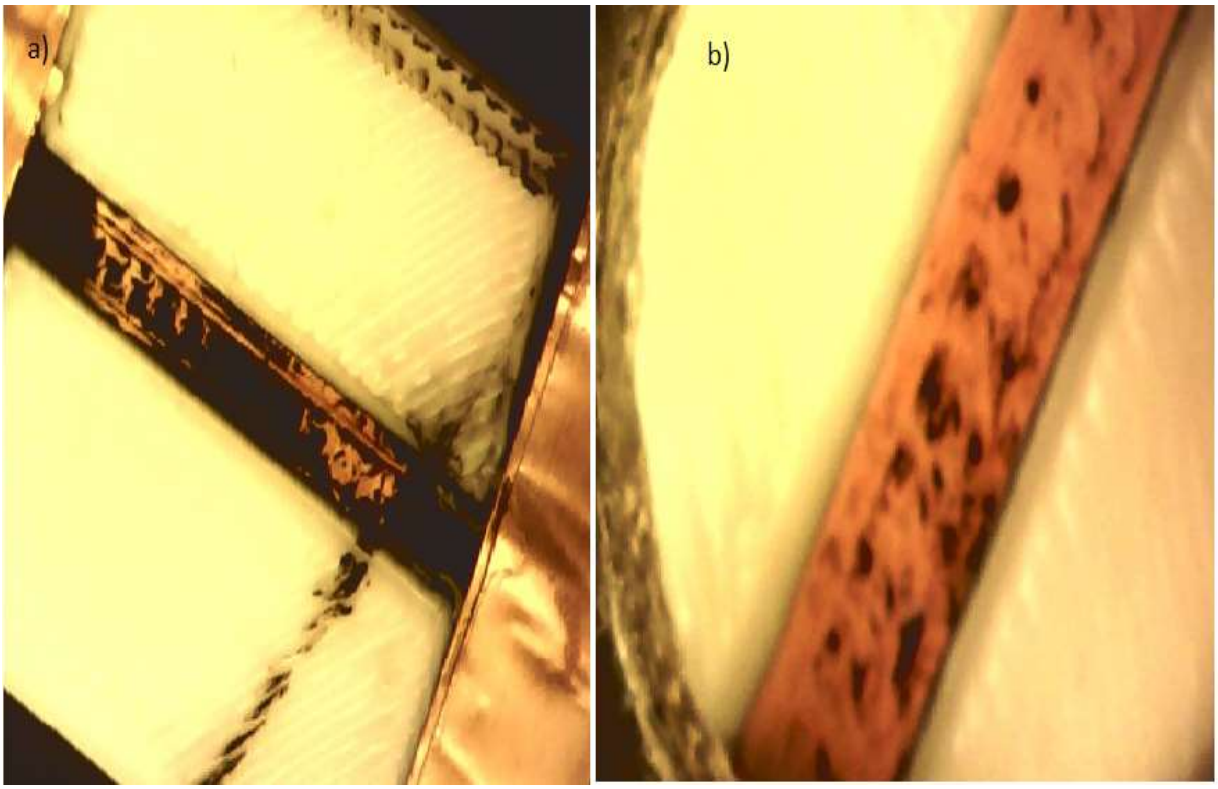

Figure 33 The Electrodeposited Sample with Two Cathode Terminals at A) 1.1V B) 1.2V

As the negative terminal was connected to both the ends of the sample, current gets doubled when compared to the current in the previous experiment with single cathode contact. The time required to deposit gets halved. Equal electrodeposition was observed on either side due to the two cathode terminals on either end of the sample. Here, we have two advantages from the new configuration. The electrodeposition layer was uniform, where the time required for electrodeposition was half the time as for regular electrodeposition at one end cathode terminal.

The electrodeposition at 1.1V was continuous along the black conductive PLA strip compared to the electrodeposition obtained by using single cathode contact as shown in Figure 12b. At 1.2V, the electrodeposition was very uniform with good adhesion strength as hydrogen evolution was not observed in this phenomenon.

4.2.1.1 Performance Characteristics

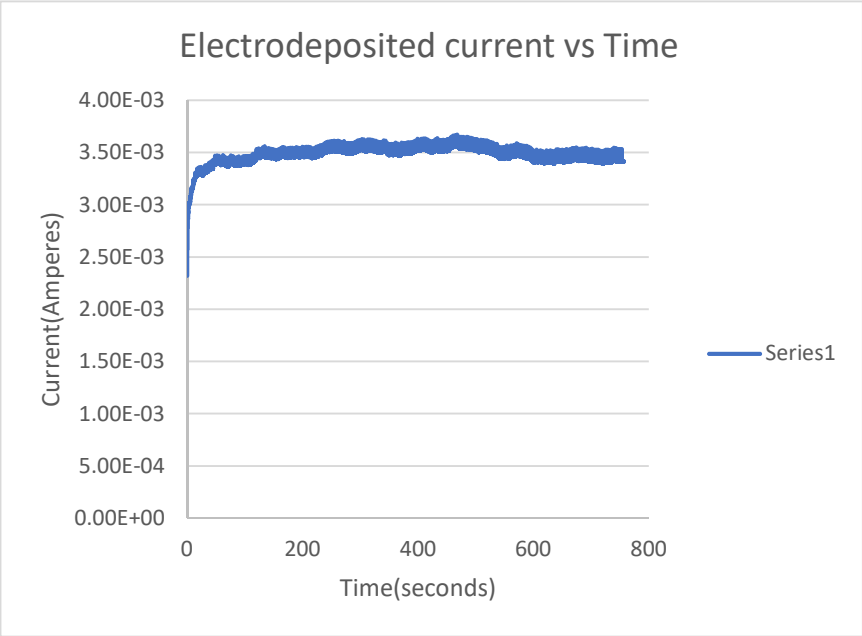

Figure 34 Electrodeposited Current vs Time at 1.1V

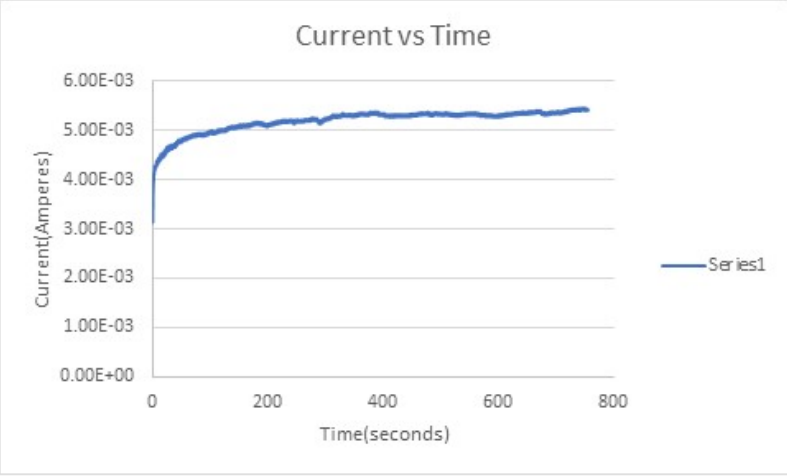

Figure 35 Electrodeposited Sample at 1.2V with Two End Cathode Terminal

From Figure 34, Figure 35, the average electrodepositing currents were approximately 3.5 mA and 5 mA. As current flows in both directions towards equal potentials, the current is two times the current at single cathode contact configuration. The currents were observed to be uniform and constant. The current density also follows the same pattern which gives a very uniform layer of deposition on 3D printed conductive substrate

Table 4 Resistance Measurements for Two Contact Configurations

Voltage(V)	Resistance by four-point probe technique(mΩ)	Resistance after peel test(mΩ)
1.1V	530	530
1.2V	35	45

4.2.1.2 Thickness and Conductivity Calculations

From Faraday's law, the relationship between current, time and weight of electroplated metal.is given by equation-5 [28].

$$W = \frac{(i \cdot t \cdot A)}{(n \cdot F)} \qquad (5)$$

where

- W= weight of electroplated metal in grams.
- i = current in Amperes.

- t=time in seconds.
- A= atomic weight of metal in grams per mole.
- n=valence of dissolved metal in solution in equivalent per mole.
- F= Faradays constant in coulombs per equivalent, F=96485.309 coulombs/equivalent.

Thickness is given by equation-6.

$$T = \frac{w \cdot 10000}{rho \cdot s} \qquad (6)$$

where

- T=thickness in microns.
- Density in grams per cubic centimeter.
- S=surface area of plated part in square centimeters.
- 10,000 is to conversion constant from centimeters to microns.

From equation 1 and 2 thickness is calculated as shown in equation-7.

$$T = \frac{(i \cdot t \cdot A \cdot 10000)}{(n \cdot F \cdot rho.S)} \qquad (7)$$

Here current and time are variables and rest of them are constants.

- The Atomic weight of copper =63.55 gm/mole.
- n=2, as Cu is plated on conductive PLA(cathode) when 2 electrons are passed through the electrolyte.
- rho=8.92 gm/cm^3, it is of a compact structure.
- S=2.250mm(breadth)*15mm (Length of electrodeposited Cu across conductive PLA strip).
- S=33.75E-2 cm^2.

Thickness for deposition of double end cathode terminal configuration is estimated as,

$$T = (1.09) * i * t \qquad (8)$$

The thickness and conductivity for common voltage configuration were calculated from simplified Equation (Equation-8) as the electrodeposited copper is continuous and uniform. The calculations were done to estimate the thickness and conductivity as shown in Table.5 and Table 6.

Table 5 Thickness Calculations

Voltages applied across sample(V)	(approximated mean current)	Time(s)	T(μm)=(1.09*i*t)
1.1	3.5 mA	795	3.04
1.2	5.1 mA	795	4.43

Conductivity is given below,

$$\text{Conductivity} = \frac{1}{\rho} \quad (9)$$

$$\rho = \frac{R.A}{l} \quad (10)$$

$$A = t \cdot w \quad (11)$$

- ρ=resistivity.
- R= Resistance (Ω).

- A=Cross sectional area(m^2).
- l=length of the electrodeposited copper strip, l=15 mm.
- t=thickness of electrodeposited copper.
- w=width of the electrodeposited copper strip, w=2.25 mm

Table 6 Conductivity Calculations.

Voltage(V)	Resistance(Ω)	Thickness(t) in m	A(m^2) =(2.25E-03) *t	$\rho = \frac{R.A}{l(0.015m)}$ (Ω-m)	Conductivity (MS/ m)
1.1	530 E-03	3.04E-06	6.84E-09	2.41E-07	4.13
1.2	35 E-03	4.43E-06	9.97E-09	2.32E-08	42.94

CHAPTER 5: CONCLUSION

The electrodeposition conducted by single cathode terminal configuration had a poor coverage of copper at low voltages. At high voltages, the hydrogen evolution effect was observed during the electrodeposition conducted by single end cathode terminal configuration. The hydrogen evolution phenomenon during electrodeposition results in good coverage of copper along the sample. When an electrodeposition was continued for longer times with hydrogen evolution effect, there were bubbles creating a very rapid growth of porous structure which leads to poor adhesion strength. The deposition of copper for shorter times with hydrogen evolution effect could be beneficial in terms of copper coverage, structure, and its adhesion strength.

The morphologies and roughness of various samples electrodeposited at different voltages were analyzed. The double end cathode terminal configuration had produced higher electroplating currents which results in good deposition rate and uniform deposition on either side of the sample. The thickness and conductivity were calculated.for the double end cathode terminal configuration.

CHAPTER 6: FUTURE WORK

A high conductive filament which can be compatible with a good resolution 3D printer (less than 100μm) can print a conductive and smooth substrate. The voltage drop due to the contact resistance and a high resistance of uncoated PLA can be avoided by a better contact probe which can directly connect to either terminal of the sample nearby overring with the high conductive substrate can improve the electrodeposition reaction process. We suggest a very small localized electroplating over ring set-up to get uniform deposition along the track. We also suggest a controlled hydrogen evolution reaction by increasing temperature.

An advanced adhesion test is also required to analyze adhesion strength of the electrodeposited copper on conductive PLA. The bridging of the surface mount device on a 3d printed conductive track can be realized using electrodeposition of copper. The aggressive growth with hydrogen evolution effect can be utilized to solder the terminals of a surface mount device.

REFERENCES

1. Falco, A., et al., Towards 3D-printed organic electronics: Planarization and spray-deposition of functional layers onto 3D-printed objects. Organic Electronics, 2016. **39**: p. 340-347.

2. Stucker, I.G.D.R.B., Additive Manufacturing Technologies 3D Printing, Rapid Prototyping, and Direct Digital Manufacturing Second Edition.

3. Rojas-Nastrucci, E.A., A.D. Snider, and T.M. Weller, Propagation characteristics and modeling of meshed ground coplanar waveguide. IEEE Transactions on Microwave Theory and Techniques, 2016. **64**(11): p. 3460-3468.

4. Ready, S., et al. 3D printed electronics. in NIP & Digital Fabrication Conference. 2013. Society for Imaging Science and Technology.

5. Jakus, A.E., et al., Metallic architectures from 3D-printed powder-based liquid inks. Advanced Functional Materials, 2015. **25**(45): p. 6985-6995.

6. Wable, G. and D. Gamota, An Update on Manufacturing with Additive Processes. Surface Mount Technology Association International, 2014.

7. Macdonald, E., et al., 3D printing for the rapid prototyping of structural electronics. IEEE Access, 2014. **2**: p. 234-242.

8. Espalin, D., et al., 3D Printing multifunctionality: structures with electronics. The International Journal of Advanced Manufacturing Technology, 2014. **72**(5-8): p. 963-978.

9. Jo, Y.H., et al., Synthesis and characterization of low temperature Sn nanoparticles for the fabrication of highly conductive ink. Nanotechnology, 2011. **22**(22): p. 225701.

10. Ahmadloo, M. and P. Mousavi. A novel integrated dielectric-and-conductive ink 3D printing technique for fabrication of microwave devices. in Microwave Symposium Digest (IMS), 2013 IEEE MTT-S International. 2013. IEEE.

11. Wang, X., et al., 3D printing of polymer matrix composites: a review and prospective. Composites Part B: Engineering, 2017. **110**: p. 442-458.

12. Boparai, K.S., et al., Development of rapid tooling using fused deposition modeling: a review. Rapid Prototyping Journal, 2016. **22**(2): p. 281-299.

13. Yeh, C.-C., Trend Analysis for the Market and Application Development of 3D Printing. International Journal of Automation and Smart Technology, 2014. **4**(1): p. 1-3.

14. Leigh, S.J., et al., A simple, low-cost conductive composite material for 3D printing of electronic sensors. PloS one, 2012. **7**(11): p. e49365.

15. Arnal, N.C., A study on 2.45 Ghz bandpass filters fabricated with additive manufacturing. 2015.

16. Monzón, M.D., et al., Process and material behavior modeling for a new design of micro-additive fused deposition. The International Journal of Advanced Manufacturing Technology, 2013. **67**(9-12): p. 2717-2726.

17. Reboul, J.-P. and G. Moussalli, About some DC conduction processes in carbon black filled polymers. International Journal of Polymeric Materials, 1976. **5**(1-2): p. 133-146.

18. Kanani, N., Electroplating: basic principles, processes and practice. 2004: Elsevier.

19. Lou, H.H. and Y. Huang, Electroplating. Encyclopedia of chemical processing, 2006. **2**: p. 839-848.

20. New World Encyclopedia contributors. Available from: http://www.newworldencyclopedia.org/p/index.php?title=Electroplating&oldid=1006773 .

21. Bard, A.J. and L.R. Faulkner, Fundamentals and applications. Electrochemical Methods, 2001. **2**.

22. Nikolić, N., et al., Morphologies of copper deposits obtained by the electrodeposition at high overpotentials. Surface and Coatings Technology, 2006. **201**(3): p. 560-566.

23. Gabe, D.R., The role of hydrogen in metal electrodeposition processes. Journal of Applied Electrochemistry, 1997. **27**(8): p. 908-915.

24. Nikolić, N.D., et al., The effect of hydrogen codeposition on the morphology of copper electrodeposits. I. The concept of effective overpotential. Journal of Electroanalytical Chemistry, 2006. **588**(1): p. 88-98.

25. Nikolić, N.D., et al., The effect of hydrogen co-deposition on the morphology of copper electrodeposits. II. Correlation between the properties of electrolytic solutions and the quantity of evolved hydrogen. Journal of Electroanalytical Chemistry, 2008. **621**(1): p. 13-21.

26. Nikolić, N.D., et al., Formation of dish-like holes and a channel structure in electrodeposition of copper under hydrogen co-deposition. Electrochimica Acta, 2007. **52**(28): p. 8096-8104.

27. Sanat, N.H., et al., Study of Thin Film Copper Electrodeposition on Carbon Substrate for Thin Film Battery Electrode Application. Journal of Science and Technology, 2016. **8**(1).

28. A california corporation., Faradays Law Available from: http://www.electrolytics.org/faradaysLaw.html.

APPENDIX A: GENERAL INFORMATION ON 3D PRINTING PROCESS

Generic AM process was explained in following steps[2].

1. Computer Aided Design software like SOLIDWORKS is used to describe the external 3D structure dimensions.
2. It should be saved as STL file in design software, as every 3D printer accepts STL file.
3. STL file can be opened in a MakerBot desktop software to make the manipulations like size, position, orientation for the building.
4. The machine should be set up with correct build parameters like infill density extruder temperature.
5. It builds on itself. Make sure filament is present.
6. Removal of printed parts after checking the plate temperature.
7. Post Processing like taking off the supporting structures should be done.
8. The application is the last step in which the printed part can be used after making requires alterations manually[2].